

Project Review Committee

Each research project will have an advisory committee appointed by the LTRC Director. The Project Review Committee is responsible for assisting the LTRC Administrator or Manager in the development of acceptable research problem statements, requests for proposals, review of research proposals, oversight of approved research projects, and implementation of findings.

LTRC appreciates the dedication of the following Project Review Committee Members in guiding this research study to fruition.

LTRC Administrator/ Manager

Chris Abadie

Members

Phil Arena, FHWA

Sam Cooper, LTRC

Mike Boudreaux, LTRC

Jason Davis, LADOTD Materials

Luanna Cambas, LADOTD

Mark Kelly, LADOTD Dist 61 Lab Engineer

David Jones, Owens Corning

Bill Daly, LSU

Delmar Soloman, Idaho Asphalt

Directorate Implementation Sponsor

LADOTD Materials

TECHNICAL REPORT STANDARD PAGE

1. Report No. FHWA/LA.04/390	2. Government Accession No.	3. Recipient's Catalog No.
4. Title and Subtitle Performance-Related Test for Asphalt Emulsions	5. Report Date October 2004	
	6. Performing Organization Code	
7. Author(s) Daniel De Kee, Ph.D., Christopher David Abadie, P.E., Max Hetzer, Graduate Research Assistant, Kyle Frederic, Undergraduate Research Assistant	8. Performing Organization Report No.	
9. Performing Organization Name and Address Tulane University Department of Chemical Engineering New Orleans, LA. 70118	10. Work Unit No.	
	11. Contract or Grant No. State Project No. 736-99-1142 LTRC Project No. 03-7B	
12. Sponsoring Agency Name and Address Louisiana Transportation Research Center 4101 Gourrier Avenue Baton Rouge, LA. 70808	13. Type of Report and Period Covered Final Report Period Covered: March 2003 - June 2004	
	14. Sponsoring Agency Code	
15. Supplementary Notes		
16. Abstract <p>Yield stress was investigated as a potential quality control parameter for asphalt emulsions. Viscometric data were determined using the concentric cylinder, parallel plate, and cone and plate geometries with rotational rheometers. We also investigated the use of a novel slotted plate technique to determine the yield stress in a direct way—that is to say, without extrapolation. The Saybolt “viscosity” was determined with a Saybolt Viscometer following the AASHTO T 72-97 standard procedure. The slotted plate technique generated reproducible and consistent results that were far superior to those obtained by rotational rheometer techniques. The yield stress of the emulsions appears to be a more accurate measure of the performance specification for asphalt emulsions than the Saybolt “viscosity” data.</p>		
17. Key Words Yield Stress, asphalt emulsions, viscometric data, rheometers, viscosity	18. Distribution Statement Unrestricted. This document is available through the National Technical Information Service, Springfield, VA 21161.	
19. Security Classif. (of this report) <p style="text-align: center;">N/A</p>	20. Security Classif. (of this page) <p style="text-align: center;">N/A</p>	21. No. of Pages
		22. Price

Performance-Related Test for Asphalt Emulsions

by

Daniel De Kee, Ph.D.
Professor of Chemical and Biomolecular Engineering
Director, Tulane Institute for Macromolecular Engineering and Science (TIMES)

Christopher David Abadie, P.E.
LTRC

Max Hetzer
Graduate Research Assistant

Kyle Frederic
Undergraduate Research Assistant

LTRC Project No. 03-7B
State Project No. 736-99-1142

conducted for

Louisiana Department of Transportation and Development
Louisiana Transportation Research Center

The contents of this report reflect the views of the author/principal investigator who is responsible for the facts and the accuracy of the data presented herein. The contents do not necessarily reflect the views or policies of the Louisiana Department of Transportation and Development or the Louisiana Transportation Research Center. This report does not constitute a standard, specification, or regulation.

October 2004

ABSTRACT

Yield stress was investigated as a potential quality control parameter for asphalt emulsions. Viscometric data were determined using the concentric cylinder, parallel plate, and cone and plate geometries with rotational rheometers. We also investigated the use of a novel slotted plate technique to determine the yield stress in a direct way—that is to say, without extrapolation. The Saybolt “viscosity” was determined with a Saybolt Viscometer following the AASHTO T 72-97 standard procedure. The slotted plate technique generated reproducible and consistent results that were far superior to those obtained by rotational rheometer techniques. The yield stress of the emulsions appears to be a more accurate measure of the performance specification for asphalt emulsions than the Saybolt “viscosity” data.

IMPLEMENTATION STATEMENT

Currently, the Saybolt test is used for quality control analysis of asphalt emulsions. With the Saybolt test procedure, the time required for 60 milliliters of a test fluid to flow through a calibrated orifice is measured. This time measurement is then associated with viscosity of the material. This procedure is reliable only when the material in question is Newtonian; the viscosity of the material is shear rate independent. The asphalt emulsions were proved to be non-Newtonian materials. The current standard Saybolt test procedure is not reliable since the shear rate that the material experiences during the test changes due to a continuously changing hydrostatic head. However, the Saybolt test procedure produces a one-point quality control parameter, which is an attractive alternative to rheological characterization involving dozens of test points.

The yield stress of multiphase materials such as asphalt emulsions is a one-point characterization parameter of the flow properties of multiphase materials. Previously, accurately determining the yield stress of materials such as asphalt emulsions was nearly impossible because of the technique involving extrapolation of viscometric data to zero shear rate. The slotted plate technique developed at Tulane University can provide accurate and reliable yield stress values of asphalt emulsions.

This report presents the results of a preliminary study to determine the feasibility of using the slotted plate technique to accurately determine the yield stress of select asphalt emulsions. The results of this study should lead to a more extensive research project that would develop a new standard quality control test for asphalt emulsions.

TABLE OF CONTENTS

ABSTRACT.....	iii
IMPLEMENTATION STATEMENT	v
TABLE OF CONTENTS.....	vii
LIST OF TABLES	ix
LIST OF FIGURES	xi
INTRODUCTION.....	1
Background	2
Emulsions.....	3
OBJECTIVE.....	5
SCOPE.....	7
METHODOLOGY	9
Saybolt and Capillary Viscometry.....	9
Rheometers.....	11
Bohlin Visco 88 Viscometer	11
Rotational Viscometers (TA Advanced Rheometer).....	11
Models for Materials that Exhibit a Yield Stress	13
Direct Yield Stress Measuring Devices	15
Vane Technique	15
Slotted Plate Technique.....	15
RESULTS AND DISCUSSION	19
Yield Stress Testing Using A New Slotted Plate Apparatus	19
Procedure.....	19
Sample SS-1	19
Sample CRS-2	20
Sample AES-300.....	21
Sample CSS-1.....	21

Sample CRS-2P.....	22
Sample AE-P.....	22
Analysis and Discussion of Slotted Plate Technique Results	23
Yield Stress Results Using Rotational Rheometers.....	24
Procedure.....	24
Results Obtained with TA AR-2000 Rheometer	25
Yield Stress Results Obtained with Bohlin 88 Viscometer.....	33
Discussion of Data Obtained via Rotational Rheometers.....	35
Saybolt Viscosity Determination of Asphalt Emulsions	36
Procedure.....	36
Results.....	36
Discussion of Saybolt Measurement Results.....	36
CONCLUSIONS	39
NOTATION	41
Greek Letters.....	41
REFERENCES	43

LIST OF TABLES

Table 1 Sample SS-1 results	20
Table 2 Sample CRS-2 results	21
Table 3 Sample AES-300 results.....	21
Table 4 Sample CSS-1 results.....	22
Table 5 Sample CRS-2P results	22
Table 6 Sample AE-P results.....	23
Table 7 Yield stress values for all samples.....	23
Table 8 Sample SS-1 results	25
Table 9 Sample CRS-2 results	26
Table 10 Sample AES-300 results.....	28
Table 11 Sample CSS-1 results.....	29
Table 12 Sample CRS-2P results	30
Table 13 Sample AE-P results.....	31
Table 14 Bohlin Visco 88 viscometer results	32
Table 15 Summary of the results for rotational rheometers and comparison with the slotted plate results.....	35
Table 16 Saybolt results	37

LIST OF FIGURES

Figure 1 Sample CRS-2P under 40X magnification.....	4
Figure 2 Saybolt viscometer	10
Figure 3 Kinematic viscometers	10
Figure 4 Slotted plate set up	16
Figure 5 Force - time curve	17
Figure 6 Sample SS-1 results	26
Figure 7 Sample CRS-2 results	27
Figure 8 Sample AES-300 results.....	28
Figure 9 Sample CSS-1 results.....	29
Figure 10 Sample CRS-2P results.....	30
Figure 11 Sample AE-P results.....	31
Figure 12 Bingham model curve fit.....	33
Figure 13 Casson model curve fit.....	34

INTRODUCTION

The rheology of suspensions and emulsions is of great interest to the industrial community since many processes involve “particles” of some kind. However, the rheological analysis of such systems is a difficult topic. The earlier models that are available to describe the rheological behavior of suspensions apply only to very dilute suspensions. Einstein’s model [1], for example, assumes a dilute suspension of rigid spheres in a Newtonian fluid, and can predict rheological behavior of suspensions only for limited cases. Einstein’s relation is given by

$$\mathbf{h}_r = \frac{\mathbf{h}}{\mathbf{h}_s} = 1 + \frac{5}{2} \mathbf{f} \quad (1)$$

where \mathbf{h}_r is the relative viscosity, \mathbf{h} is the viscosity of the suspension, \mathbf{h}_s is the solvent viscosity, and \mathbf{f} is a volume fraction occupied by the spheres. Einstein’s theoretical result is only valid for very low concentrations ($\mathbf{f} < 0.01$).

Larson [2] considers the simplest case of a steady flow of a dilute suspension of Newtonian drops or bubbles in a Newtonian medium through a capillary. If the capillary number,

$$Ca = \mathbf{h}_s \dot{\mathbf{g}}_{rz} a / \Gamma \quad (2)$$

with (a) being the surface area and (Γ) the surface tension of the solvent, is small, the drops or bubbles do not deform under flow and the suspension viscosity at a steady state is given by Taylor’s extension of the Einstein formula for solid spheres:

$$\mathbf{h}_r \equiv \frac{\mathbf{h}}{\mathbf{h}_s} = 1 + \frac{1 + \frac{5}{2}M}{1 + M} \mathbf{f} \quad (3)$$

where M is the ratio of the viscosities of the dispersed to the suspending fluids. As $M \rightarrow \infty$, the droplets behave like hard spheres, and Einstein’s result is recovered. As $M \rightarrow 0$, the relative viscosity is lower, $\mathbf{h}_r = 1 + \mathbf{f}$, which is generally true for bubbles. The viscosity of a suspension of bubbles is less than that of a suspension of hard spheres at a given volume fraction because liquid

bounding the surface of a bubble can flow. Hence, bubbles disturb the flow field of the external fluid less than do hard spheres [2].

Some researchers found that the viscosity of suspensions containing two types of solid particles exhibit a decrease in viscosity [3, 4]. Goto and Kuno determined that the relative viscosity of the suspension of a single component was lowered by mixing particles of different sizes [3]. The relative apparent viscosity of the suspension was at a minimum when the volume fraction for the larger particles with respect to the total solids was about 60 percent. Also, the possible lubrication effect by small particles was observed. Hoffman observed that as the size of the particles in the suspension decreased, the viscosity of the suspension rose exponentially as the number of particles increased [4]. The suspension became strongly shear thinning for $f > 0.35$; Van Der Werff and De Kruif, showed similar behavior for four submicron sterically stabilized silica dispersions with differing particle sizes [5]. They found that the high and low shear limiting viscosities are functions of the volume fraction only, and the volume fraction at which the viscosity diverges is independent of the particle size. Note that asphalt emulsions are dispersions of droplets with a wide size distribution.

We investigated the use of the yield stress value to characterize asphalt emulsions and to possibly replace the Saybolt grading procedure with the emulsion yield stress, which should be a more accurate quality control tool. Materials such as suspensions, coatings, and emulsions possess a three-dimensional microstructure, which imparts solid-like properties but is susceptible to structural breakdown under an applied force [1]. The flow properties of these materials are between those of a solid and a liquid. When the material is subjected to a small stress, it behaves as a solid. However, when this stress is large enough, the sample behaves as a liquid and begins to flow. Ketchup is a well known example of a yield stress material (yield stress value is 15 Pa for Heinz 57 ketchup). If the ketchup bottle is turned over, the ketchup will not flow until sufficient force is applied. Yield stress is defined as the minimum amount of force that must be applied to degrade a material's structure and induce flow. It is important that any multiphase material of industrial significance be accurately characterized by this critical control parameter, as the yield stress can play an important role in determining the processing constraints during production, storage, transportation, and overall performance of the product [6].

Background

Emulsions

An emulsion is defined as a stable dispersion of one liquid in a second immiscible liquid [7].

Furthermore, an asphalt emulsion is a combination of three main substances: asphalt, water, and a small amount of an emulsifying agent or “soap” that stabilizes the emulsion [8]. One of the asphalt models has been proposed by Kennedy and Cominsky [9], who considered an asphalt emulsion as a suspension of aromatic, high-molecular weight, core molecules dispersed in a medium of relatively low-molecular weight molecules. The dispersed phase is viewed as being peptized by absorbed aromatic molecules lower in molecular weight than the core materials, which are soluble in the dispersing medium. The core materials are considered to be asphaltene micelles, the peptizing agents are considered to be resins, and the dispersing media are considered to be oils (maltenes).

Kennedy and Cominsky’s [9] working hypothesis of the asphalt structure states that the phase consisting of relatively aliphatic, non-polar molecules that are low in heteroatoms disperses the micellar structures of asphaltene-like molecules. These asphaltene-like molecules are aromatic, polar, and contain heteroatom functional groups. The size of the micelles may vary widely, but for emulsion CRS-2P the largest droplet size was 95 μm , and the average droplet size was 65 μm . Some asphalt emulsions have an observable amount of micellar structures that are small in size and number, are well dispersed, and exhibit Newtonian behavior [10]. Other asphalt emulsions contain substantial amounts of poorly dispersed large micelles and are capable of forming three-dimensional networks of asphaltene micelles within the emulsion, thus exhibiting non-Newtonian behavior [10].

The four most important components of asphalt are oil, crystallizable waxes, resin, and asphaltenes. The oil fraction of asphalt includes structures of fused naphthenic rings with linear and branched aliphatic side chains of various lengths. The resin fraction of asphalt consists of hundreds of different hydrocarbons, but the general nature of resin fraction consists of polycyclic molecules containing saturated aromatic, heteroaromatic rings and heteroatoms in various functional groups [11].

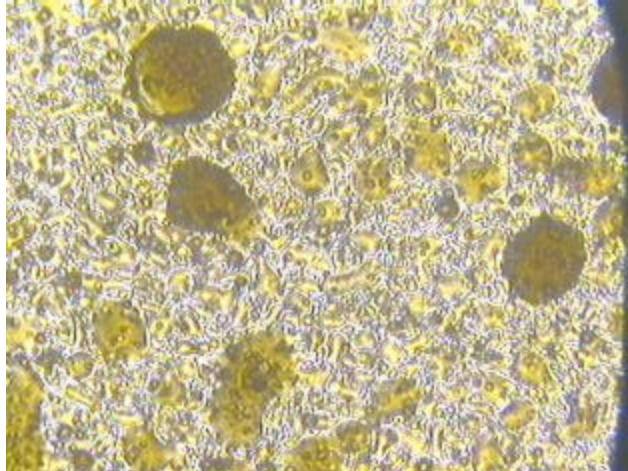


Figure 1
Sample CRS-2P under 40X magnification, 1 cm = 100 μ m

These components are sheared in a high-speed mixer called a colloid mill that produces tiny asphalt droplets. The emulsifier, which is a surface-active agent, keeps the asphalt droplets in a stable emulsion. The result is a liquid product with a consistency ranging from that of milk to heavy cream, which can be used in cold processes for road construction and maintenance.

Asphalt emulsions can be classified into three categories that refer to the electrical charges surrounding the asphalt particles: anionic, cationic, or nonionic. They are further classified on the basis of how quickly they coalesce; that is, how quickly they form asphalt cement [8].

Many advantages result from using asphalt emulsions. Asphalt emulsions do not require a petroleum solvent to liquefy, and they can usually be used without applying additional heat. Both of these factors contribute to energy savings. Additionally, asphalt emulsions are environmentally friendly. Hardly any hydrocarbon emissions are created by their use [8]. Because of their environmental properties, energy efficiency, and cost effectiveness, emulsions will likely emerge as the asphalt product of the future for pavement maintenance, roofing, and specialty industrial applications [8, 12]. Choosing the right emulsion and application technique yields substantial economic and environmental benefits [13].

OBJECTIVE

This initial research project characterized several different samples of asphalt emulsions and compared the results from different types of rheological tests. Several testing procedures were used for this project to reveal some rheological characteristics of the emulsions. The novel slotted-plate technique, measurements using coaxial cylinder geometry (Bohlin Visco 88 rheometer), Saybolt viscometer testing, as well as cone and plate and parallel plate geometries (TA AR2000 rheometer) were performed to identify the sample yield stress and viscosity functions.

SCOPE

Six samples of asphalt emulsions provided by LTRC were tested with the slotted plate technique at 25°C. The 2ⁿ factorial test design was used to determine the effects of several variables on the yield stress of emulsions. The maximum test time was optimized to be less than 30 minutes in order to be comparable to the Saybolt test procedure.

The viscometric data was determined with the TA AR-2000 rheometer and Bohlin Visco 88 viscometer. The data was fitted to Bingham and Casson models to determine the yield stress value of the emulsion samples. The temperature was kept constant at 25°C, and the sample preparation procedure was same as for the slotted plate technique.

The Saybolt data was obtained at the LDOT 2 Lab, using the AASHTO T 72-94 standard procedure. The data was analyzed with MS Excel and then used to determine the quality of the asphalt emulsions samples.

METHODOLOGY

Saybolt and Capillary Viscometry

Rheological properties, such as viscosity, are measured via rheometers such as the Bohlin Visco 88 rotational viscometer, the Saybolt viscometer, and/or the TA AR-2000 advanced rheometer. One can obtain qualitative information about the flow characteristics of a Newtonian fluid by measuring the time required for a fixed volume of a fluid (at a given temperature) to flow through a calibrated orifice or capillary tube. Note that such a measurement is not associated with viscosity units, which are $Pa \cdot s$ in SI units. Several types of viscometers are used today. The Saybolt viscometer shown in figure 2 is used to determine the viscosity of Newtonian fluids. It consists of four cylinders (sample holders) of equal volume with capillary outlet tubes at the bottom of the cylinders. The cylinders are immersed in a constant temperature bath. The sample is loaded in the cylinders and allowed to reach thermal equilibrium. Then the fluid is allowed to flow through an orifice (capillary) and the efflux time, which is the time required for 60 milliliters of fluid to flow through the capillary, is recorded.

The sample is stirred by a mixer prior to a measurement to achieve a similar initial structure and generate reproducible results. The time measured is used to express the fluid's viscosity in Saybolt Universal Seconds or Saybolt Furol Seconds. (Note: the asphalt emulsions are always measured in Saybolt Furol Seconds.)

$$\mathbf{n} = Ft \tag{4}$$

Where \mathbf{n} is the kinematic viscosity of the fluid expressed in seconds, F is the calibration constant of the orifice (capillary), and t is the efflux time. The calibration constant is determined for each orifice using a standard with a known viscosity.

The glass capillary viscometers, shown in figure 3, are examples of a second type of viscometer. These viscometers are used to measure kinematic viscosity. Like the Saybolt viscometer, a glass capillary is used to measure the time in seconds required for the test fluid to flow through a bulb. This time is multiplied by a temperature constant, determined from the calibration of the tube in use, to provide the viscosity expressed in centistokes.



Figure 2
Saybolt Viscometer

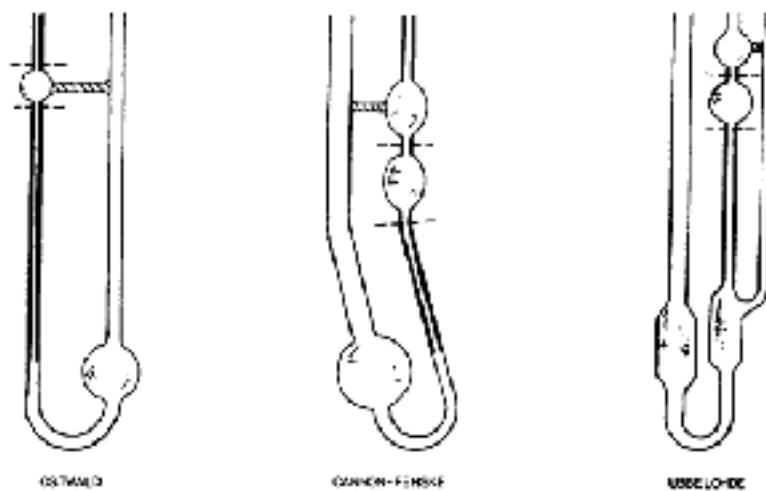


Figure 3
Kinematic Viscometers

Rheometers

Bohlin Visco 88 Viscometer

The portable and easy-to-use Bohlin Visco 88 viscometer uses coaxial cylinder geometry. In this study, the sample was prepared the same way as a Saybolt test sample. The sample was loaded until the thermocouple was slightly immersed. A range of shear rates was chosen, and shear stress versus shear rate data was plotted; the yield stress was determined with an extrapolation procedure from the obtained viscometric data.

Coaxial Cylinder Geometry. Most modern rheometers are rotating devices that can rapidly determine the viscosity curve as well as other important rheological material functions. Commercial rheometers are available with computer control and software packages for data analysis. The measurements are made using three possible geometries: coaxial cylinders, cone and plate, and parallel plates. Coaxial cylinders were the first rotating devices used to measure viscosity. Basically, the geometry consists of a stationary cylinder and a rotating cylinder. The sample is loaded in the gap between the cylinders, which should be small to approximate a constant shear rate. Depending on the setup, either the inner or outer cylinder rotates. After the torque is measured, the viscosity can then be calculated [1].

Rotational Viscometers (TA Advanced Rheometer)

The TA AR2000 advanced rheometer is a powerful and versatile research-grade rheometer. This instrument utilizes different measuring system geometries than used with the Bohlin 88 viscometer. Parallel-plate and cone and plate geometries are used.

Cone and Plate Geometry. The cone and plate geometry is the most popular for determining the viscosity of viscoelastic fluids. A small sample is placed in the space between a plate of radius R and a cone of the same radius with a very small angle, so that the shear rate is constant in the gap. The sample should have a free spherical-shaped surface at the outer edge. For viscous fluids, the cone can be positioned below the plate, and either the cone or the plate can be rotated. The shear stress can be determined from the measured torque as follows:

$$T = 2\mathbf{p} \int_0^R \mathbf{s}_{qf} r^2 dr = \frac{2}{3} \mathbf{p} R^3 \mathbf{s}_{qf}$$

(5)

where T is the torque, \mathbf{s}_{qf} is the shear stress, and $\dot{\mathbf{g}}_{qf}$ is the shear rate

From

$$\mathbf{s}_{qf} = -\mathbf{h}\dot{\mathbf{g}}_{qf} \quad (6)$$

where

$$\dot{\mathbf{g}}_{qf} \approx -\frac{\Omega}{q_0} \quad (7)$$

where q_0 is the cone angle; the non-Newtonian viscosity is given by

$$\mathbf{h} = \frac{3q_0T}{2pR^3\Omega} \quad (8)$$

The torque (T) is measured and the rotational velocity (Ω) is controlled [1].

Determining rheological properties does not require any assumption about flow kinematics, nor does it require the rheological models. Very small sample volumes are needed. The system allows for very good heat transfer and temperature control. End effects are negligible, at least for low rotational speeds when using the appropriate quantity of fluid in the gap.

While this geometry appears to be ideal for rheological studies, it does have some disadvantages. The system is limited to low shear rates, especially for highly elastic systems which would not stay in the gap at a high rotational speed. It is difficult to eliminate evaporation and free-boundary effects for solutions involving volatile solvents. Highly erroneous results are possible for multiphase systems such as suspensions of solids and polymer blends, in which the particles or domain sizes are of the same order of magnitude as the gap size [1].

Parallel-Plate Geometry. Since the cone and plate geometry may not be ideal for the study of multiphase system and polymer blend rheology, the parallel-plate geometry can be used.

This geometry consists of two parallel concentric discs of radius R with a constant separation or gap. One of the plates rotates and the other remains stationary; the torque and normal thrust can be measured at either plate. The edge represents a free boundary on the measured torque and axial forces are usually negligible. This geometry is advantageous for high temperature measurements, particularly when multiphase systems are studied. The gap can be varied to accommodate a variety of particle sizes.

For a small gap ($h/R \ll 1$), or for low rotational speed, the velocity profile for steady-state conditions is given by

$$V_q = \Omega r \left(1 - \frac{z}{h} \right) \quad (9)$$

and the shear rate ($\dot{\mathbf{g}}_{zq}$) is given by

$$\dot{\mathbf{g}}_{zq} = \Omega \frac{r}{h} \quad (10)$$

Carreau et. al [2], state that for non-Newtonian fluids, the viscosity is no longer proportional to the torque because the shear rate varies with the radial position. The viscosity for non-Newtonian fluids can be expressed by the following equation:

$$h(\dot{\mathbf{g}}_R) = \frac{T}{2pR^3 \dot{\mathbf{g}}_R} \left[3 + \frac{d \ln \left(\frac{T}{2pR^3} \right)}{d \ln \dot{\mathbf{g}}_R} \right] \quad (11)$$

Models for Materials That Exhibit a Yield Stress

Bingham Model. The Bingham model is the simplest one to use because it is a straightforward extension of Newton's law of viscosity:

$$\left\{ \begin{array}{ll} \mathbf{s}_{yx} = -h_0 \dot{\mathbf{g}}_{yx} \pm \mathbf{s}_0 & \text{if } |\mathbf{s}_{yx}| > |\mathbf{s}_0| \\ \dot{\mathbf{g}}_{yx} = 0 & \text{if } |\mathbf{s}_{yx}| \leq |\mathbf{s}_0| \end{array} \right\} \quad (12)$$

The parameters are \mathbf{s}_0 and \mathbf{h}_0 . The model indicates that the sample behaves like a Newtonian material when the shear stress exceeds the yield stress \mathbf{s}_0 , and it doesn't flow when the shear stress is less than the yield stress [1].

Casson Model. The Casson model is given by

$$\sqrt{|\mathbf{s}_{yx}|} = \sqrt{\mathbf{s}_0} + \sqrt{\mathbf{h}_0 |\dot{\mathbf{g}}_{yx}|} \quad (13)$$

A plot of $\sqrt{|\mathbf{s}_{yx}|}$ versus $\sqrt{|\dot{\mathbf{g}}_{yx}|}$ will produce $\sqrt{\mathbf{s}_0}$ as intercept.

Both models introduce a yield stress value; however, the assumption is that the sample behaves as a Newtonian fluid at low shear rates.

Direct Yield Stress Measuring Devices

Vane Technique

One of the direct yield stress measuring devices involves a vane, which generally consists of a small number (2-8) of blades arranged at equal angles around a small cylindrical shaft. In addition to the elimination of wall slip, this geometry can keep any disturbance caused by the introduction of the vane into the sample to a minimum.

A vane test is done by gently introducing the vane spindle into a sample of the suspension held in a container until the vane is fully immersed. The vane is then rotated very slowly at a constant rotational speed, and the torque required to maintain the vane's constant motion is measured as a function of time [14]. From the resulting torque-time curve, the maximum torque that corresponds to the point at which the sample begins to flow can be determined; i.e. the yield stress point. The following correlation between torque and yield stress was derived by Nguyen and Boger [14]:

$$T_m = \frac{\rho D_v^2}{2} \left(\frac{H}{D_v} + \frac{1}{3} \right) \mathbf{s}_0 \quad (14)$$

where T_m is the torque, \mathbf{s}_0 is the yield stress, D_v and H are the dimensions of the vane.

It is assumed that the \mathbf{s}_e (shear stress at the end surface) is uniformly distributed over both end surfaces of the vane and that \mathbf{s}_e is equal to the shear stress $\{\mathbf{s}_w (= \mathbf{s}_{r\theta} |_{r=R_v})\}$. Also, at the maximum torque (T_m), it is assumed that the material yields instantaneously along the virtual cylindrical surface described by the vane rotation, and that the shear stress \mathbf{s}_w is equal to the material yield stress \mathbf{s}_0 .

Slotted plate technique

Setup. A direct yield stress measuring device was constructed by Zhu and De Kee [6]. This instrument, shown in figure 4, employs a slotted plate, which unites the advantages of both vane and solid plate direct yield stress measurements. It is not restricted by the assumptions of the vane method and eliminates the wall effect present with the solid plate method.

The slotted-plate technique consists of a linear motion platform (Applied Motion Products) driven by a step motor (Si3540 programmable step motor driver), a balance (Ohaus, AP250D, capacity

52/210g, resolution 0.01/0.1 mg), and a controlling computer. This computer controls the speed of the platform. A second computer is connected to the balance via a serial connection through the COM1 port for data analysis. A piece of thread hangs from the balance, and a thin stainless steel wire (0.127 mm in diameter) is connected to the thread. This eliminates the torque exerted on the plate, which is connected to the wire, from influencing the balance reading.



Figure 4
Slotted plate set up

Procedure. The samples were stirred by a mixer prior to measurement in order to achieve a similar initial structural state. After the mixing, the asphalt emulsion was loaded into a plastic beaker, placed on the platform, and allowed to rest for two minutes. The slotted plate was suspended from the balance and vertically inserted into the sample at point A in figure 5. A 15-minute rest period at this point allowed the system to equilibrate. A 10- μ l drop of water-soluble surfactant (Tween 85) was placed on the sample surface (point B in figure 5). Once the force versus time curve plateaued (point C in figure 5), the platform was lowered at a controlled and constant rate. As the platform was lowered, the sample in the beaker exerted a force on the plate. This continuously changing force was recorded by the balance and plotted in Excel as a force versus time curve. Once the acting force exceeded the sample yield stress (change in slope), flow began in

the vicinity of the plate, where the stress had the largest magnitude (point D in figure 5). Point C refers to the “initial force” (F_i), and point D is the force (F) at time t_r .

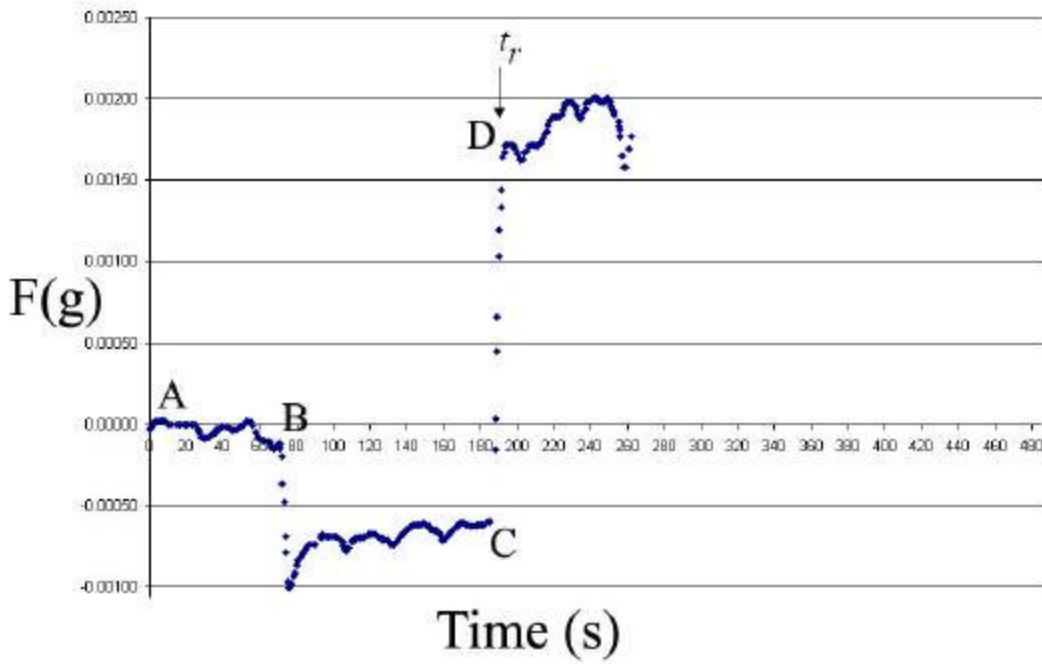


Figure 5
Force - time curve

This point is characterized by a change in slope at $t = t_r$. The yield stress is given by:

$$s_0 = \frac{F_r}{S} = \frac{F - F_i}{S} \quad (15)$$

where S is the total surface area of the plate, F is the total force obtained by the balance at time t_r , and F_i is the measured initial force.

RESULTS AND DISCUSSION

Yield Stress Testing Using a New Slotted Plate Apparatus

Procedure

The sample was first rotated on the CEL-GRO Rotator for at least 24 hours at 7 rpm to ensure the consistency of the sample. The samples used for these tests were stored for an extended period of time and needed to be homogenized before the testing was performed. In a field situation, this step can be neglected because the samples would be homogenized while in transport.

After rotating for 24 hours or more, a sample was poured into a 100 ml beaker and mixed by hand to remove any air bubbles that formed on the surface. The sample was allowed to rest for two minutes before inserting the plate. After the plate was vertically inserted in the sample, the system was allowed to equilibrate. Allowing the sample to rest for 2 and 15 minutes before starting the motor determined the time needed for the emulsion to achieve equilibrium. After inserting the plate, the data collecting software (Winwedge), together with an Excel file, recorded the data from the balance. After the curve plateaued, 10 μ L of surfactant (Tween 85) was added to the sample's surface. The need for surfactant arises when the yield stress of the material is of the same or lower magnitude than the surface tension force at the stainless steel wire – surface interface. The surfactant is a surface acting agent and will stay on the surface of the emulsion if the surfactant concentration is small. We added 10 μ L of surfactant, which is small enough for us to be confident that the surfactant will not interact with the emulsion. After the curve plateaued again, the motor was started (rate of lowering is 0.025 mm/s) and the data was recorded. The results indicated that the surfactant was not necessary. (Note: all tests were performed at 25°C.)

Sample SS-1

The average yield stress was determined to be 0.011 Pa. A 2^n factorial design testing procedure was followed, where $n = 3$ with the mixing time (min.), mixing speed (rpm), and the rest time after mixing (min.) as variables. This factorial design procedure was chosen to determine the effect of the aforementioned variables on the yield stress of the asphalt emulsions. We used an industrial mixer (Silverson L4RT) with variable speed control to mix the sample before the plate was inserted. The yield stress results are given in table 1.

Table 1
Sample SS-1 results

Mixing Time (min.)	Mixing Speed (rpm)	Rest Time after Mixing (min.)	Average Yield Stress (Pa)
2	100	2	0.012
2	100	15	0.011
2	1000	2	0.010
2	1000	15	0.011
15	100	2	0.011
15	100	15	0.010
15	1000	2	0.011
15	1000	15	0.011
Average			0.011

The results show that the mixer had no significant effect on the yield stress of the emulsions. Thus, the rest of the samples were not mixed with the mixer but were mixed by the CEL-GRO Rotator for 24 hours and by hand for two minutes. Again, this mixing procedure will be modified for field testing.

Sample CRS-2

The average yield stress was 0.035 Pa. A 2² factorial design testing procedure was followed, since mixing speed was determined to be of little significance. The variables were rest time after mixing (min.) and rest time (min.) after plate insertion. The yield stress results for sample CRS-2 are given in table 2.

Table 2
Sample CRS-2 results

Rest Time After mixing (min.)	Rest Time After plate insertion (min.)	Yield Stress (Pa)
2	2	0.033
2	15	0.034
15	2	0.035
15	15	0.035
Average		0.035

Sample AES-300

The average yield stress was 0.204Pa. Again, a 2² factorial design testing procedure was followed, since mixing speed was determined to be of little significance. The variables were rest time after mixing (min.) and rest time (min.) after plate insertion. The yield stress results for sample AES-300 are given in table 3.

Table 3
Sample AES-300 Results

Rest Time After Mixing (min)	Rest Time After Plate Insertion (min)	Yield Stress (Pa)
2	2	0.197
2	15	0.204
15	2	0.201
15	15	0.209
Average		0.203

Sample CSS-1

The average yield stress was 0.052 Pa. The procedure outlined for sample CRS-2 was used to determine the yield stress. The yield stress results for sample CSS-1 are given in table 4.

Table 4
Sample CSS-1 results

Rest Time After Mixing (min)	Rest Time After Plate Insertion (min)	Yield Stress (Pa)
2	2	0.050
2	15	0.053
15	2	N/A ¹
15	15	0.054
Average		0.052

¹ The data is unavailable for this test due to the shortage of materials

Sample CRS-2P

The average yield stress was 0.033 Pa. The procedure outlined for sample CRS-2 was used to determine the yield stress. The yield stress results for sample CRS-2P are given in table 5.

Table 5
Sample CRS-2P results

Rest Time After Mixing (min)	Rest Time After Plate Insertion (min)	Yield Stress (Pa)
2	2	0.031
2	15	0.029
15	2	0.033
15	15	0.037
Average		0.033

Sample AE-P

The average yield stress was 0.0016 Pa. The procedure outlined for sample CRS-2 was used to determine the yield stress. The yield stress results for sample AE-P are given in table 6.

Table 6
Sample AE-P results

Rest Time After Mixing (min)	Rest Time After Plate Insertion (min)	Yield Stress (Pa)
2	2	0.0011
2	15	0.0017
15	2	0.0016
15	15	0.0015
Average		0.0015

Analysis and Discussion of Slotted Plate Technique Results

The two-minute rest time after insertion was insufficient for samples CRS-2, CRS-2P, and CSS-1 to achieve a steady state, thus rendering the yield stress determinations inaccurate. Those samples need at least 13 minutes to come to equilibrium. A 15-minute rest period after plate insertion in the sample is sufficient to determine the yield stress accurately.

Table 7
Yield Stress Values for All Samples

	SS-1	CRS-2	AES-300	CSS-1	CRS-2P	AE-P
Yield stress (Pa)	0.011	0.035	0.203	0.052	0.033	0.0016
Average % Error (%)	2.51	1.9	0.87	1.38	5.60	5.83
Standard Deviation	0.0008	0.0011	0.0049	0.0019	0.0052	0.0002

The average yield stress values and percent error for the samples are given in the table 7. The factorial experimental design procedure showed that the mixer speed and time of mixing had no significant effect on the yield stress of sample SS-1. A rest time of two minutes was observed before the insertion of the plate to allow the sample to come to equilibrium. Different rest times after plate insertion did not have a substantial effect on the yield stress for this sample. From the data it is clear that the test can be performed within two minutes after inserting the plate in the sample SS-1.

For sample CRS-2 the variables were the rest time after mixing and rest time after plate insertion. It was assumed that neither the mixing time nor the rate of mixing had a significant effect on the yield stress of the sample. The average percent error for this set of data is 1.9 percent, which is well within an acceptable error range. The rest times after mixing and after plate insertion did not have a

significant effect on the yield stress results. The yield stress results varied less in the longer rest times after plate insertion than in the shorter rest times. This observation suggests that the sample requires more than two minutes to achieve equilibrium. Thus the suggested rest time is at least five minutes for sample CRS-2.

For the rest of the samples, the variables remained the same: the rest time after mixing, and the rest time after plate insertion into the sample. Both variables were tested for two and fifteen minutes following the 2^2 factorial test design. It was found that the two-minute rest time after insertion of the plate was not sufficient for most samples to come to equilibrium, and the rest time before the insertion of the plate into the sample (the time after mixing) had no significant effect on the yield stress determinations of the sample. Different charges on particles in samples CSS-1 and SS-1 would create different structures, leading to different yield stress values. We have noted that CRS-2P is settling faster than AE-P, likely contributing to the larger percent error.

Yield Stress Results Using Rotational Rheometers

Procedure

The sample was prepared as described earlier. The sample was loaded into the TA AR2000 advanced rheometer using a parallel plate or cone and plate geometry, depending on the sample. The CRS-2 samples were tested with parallel plate geometry since the particle size was larger than the minimum gap associated with the cone and plate geometry. The sample was allowed to rest for five minutes before testing. The TA AR2000 software computed the data. Testing via concentric cylinder geometry was performed with a Bohlin 88 viscometer. The sample was loaded into the cap and the rotational cylinder was immersed in the sample. Again, the sample was allowed to rest for five minutes prior to the start of the experiment. All tests were performed at 25° C.

Results Obtained with TA AR-2000 Rheometer

Sample SS-1. The data obtained for the sample SS-1 via the rotational measurements are shown in figure 6. The computed Casson and Bingham yield stress values are shown in table 8, along with the slotted plate results. The extrapolations used the data at the lower values of shear rate. Clearly, using all of the viscometric data for the extrapolation process would result in even larger errors.

Table 8
Sample SS-1 results

	Bingham Yield Stress (Pa)	Casson Yield Stress (Pa)	Slotted Plate Yield Stress (Pa)
Trial 1	0.100	0.012	0.012
Trial 2	0.200	0.063	0.010
Trial 3	0.050	0.012	0.011
Average	0.117	0.029	0.011
Percent Error (%)	24.67	39.79	2.51

The three tests produced three different curves at the low shear rate values; values at low shear rate are required in order to extrapolate to zero shear rate. At higher shear rate values, the three curves converged. The Bingham model assumes Newtonian behavior of the sample, once the sample starts flowing. Note that the SS-1 samples were non-Newtonian fluids, further adding to the difficulties encountered by determining the material yield stress via an extrapolation technique.

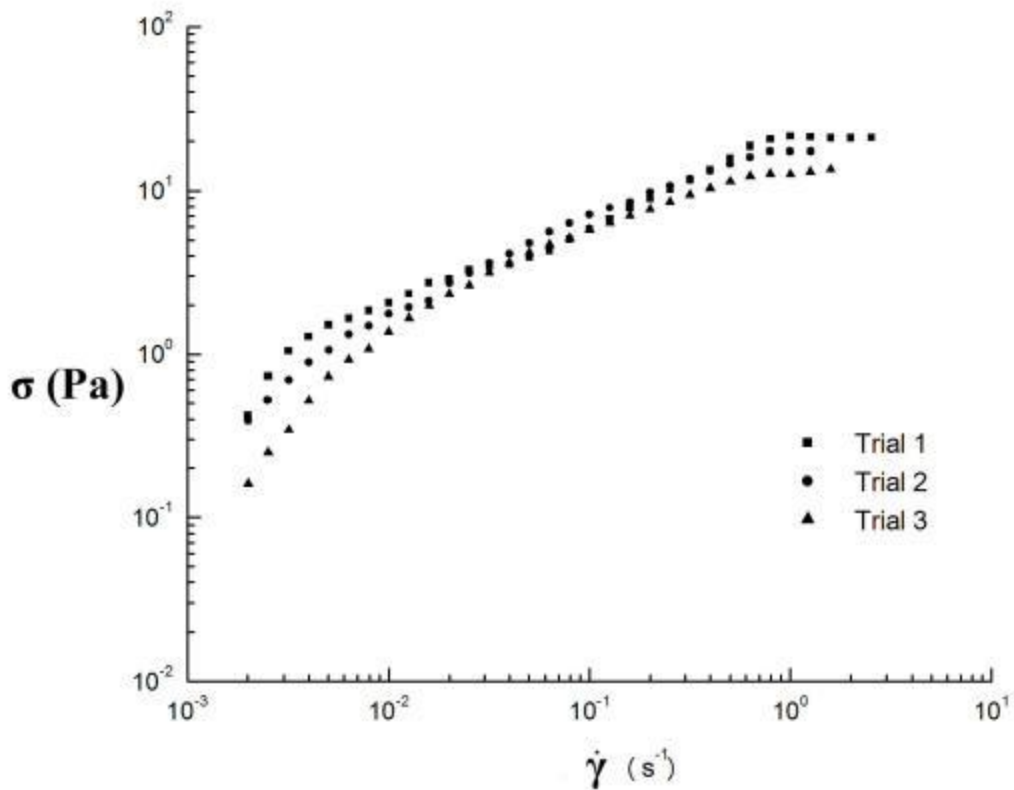


Figure 6
Sample SS-1 results

Sample CRS-2. The data obtained for the sample CRS-2 via the rotational measurements are shown in figure 7. The computed Casson and Bingham yield stress values are shown in table 9, along with the slotted plate results.

Table 9
Sample CRS-2 results

	Bingham Yield Stress (Pa)	Casson Yield Stress (Pa)	Slotted Plate Yield Stress (Pa)
Trial 1	0.130	0.036	0.035
Trial 2	0.150	0.078	0.034
Trial 3	0.450	0.303	0.035
Average	0.243	0.139	0.035
Average Percent Error (%)	27.96	41.23	1.95

The extrapolations used the data at the lower values of shear rate. Clearly, using all of the viscometric data for the extrapolation process would result in even larger errors. Here again, the shear stress response varied greatly from trial to trial in the low shear rate region, which is the region of interest. At higher shear rate values, the curves converged. Clearly, the data from the extremely low shear rate region are not reliable.

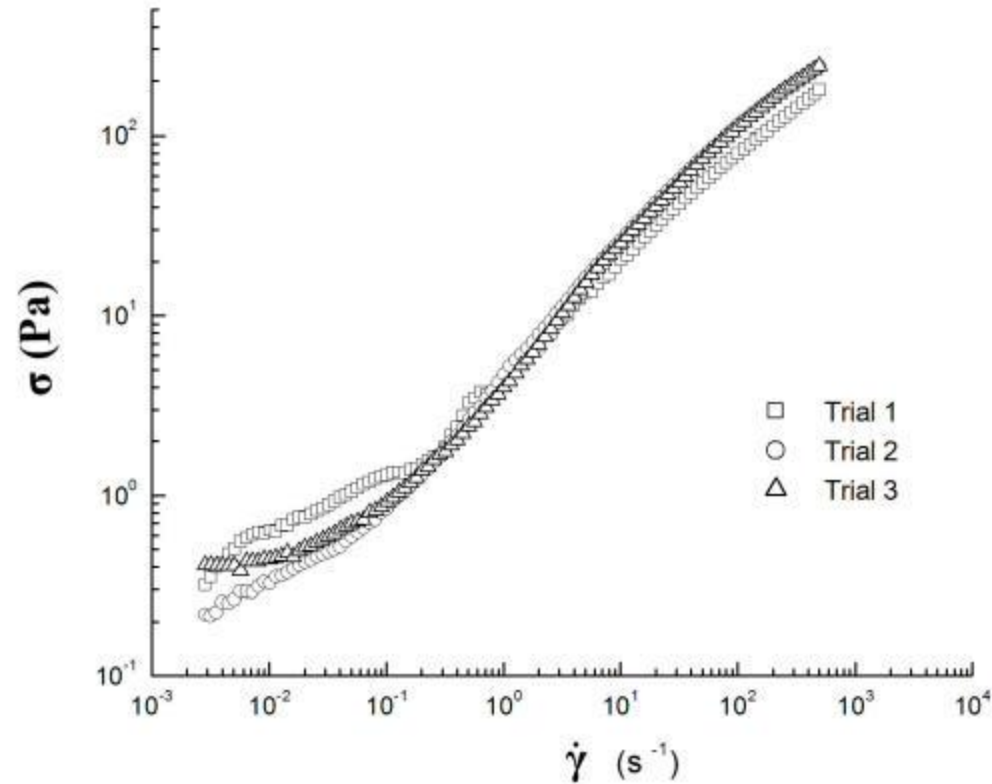


Figure 7
Sample CRS-2 results

Sample AES – 300. The data obtained for the sample AES-300 via the rotational measurements are shown in figure 8. The computed Casson and Bingham yield stress values are shown in table 10, along with the slotted plate results.

Table 10
Sample AES-300 results

	Bingham Yield Stress (Pa)	Casson Yield Stress (Pa)	Slotted Plate (Pa)
Trial 1	0.051	0.040	0.204
Trial 2	1.200	0.160	0.201
Trial 3	0.048	0.036	0.209
Average	0.433	0.079	0.205
Average Percent Error (%)	68.65	34.47	0.705

Again, the extrapolations used the data at the lower values of shear rate. Not surprisingly, the data in the ($<10^{-2} \text{ s}^{-1}$) shear rate region varied greatly from trial to trial; this was no longer true of the higher shear rate values.

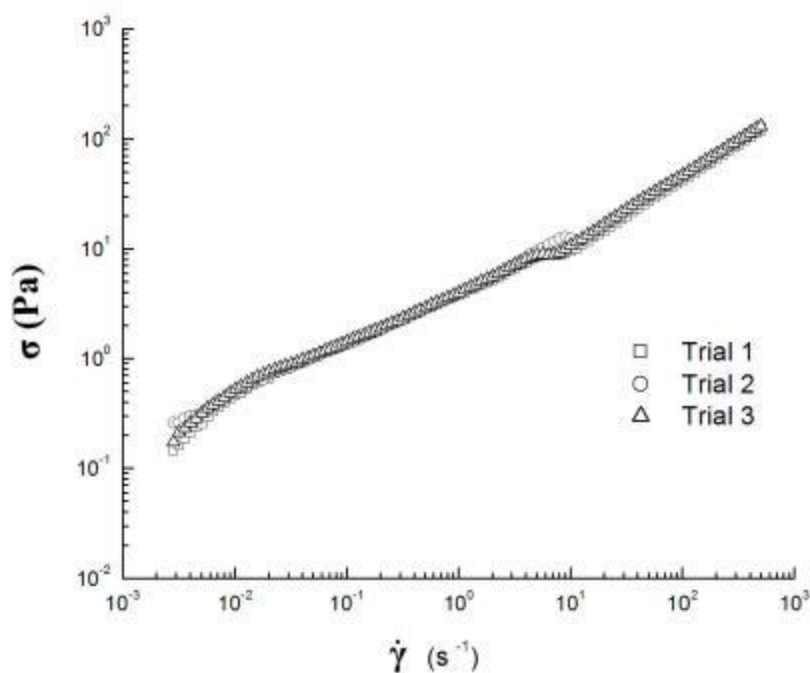


Figure 8
Sample AES-300 results

Sample CSS – 1. The data obtained for the sample CSS-1 via the rotational measurements are shown in figure 9. The computed Casson and Bingham yield stress values are shown in table 11, along with the slotted plate results. Again, the extrapolations used the data at the lower values of shear rate.

Table 11
Sample CSS-1 results

	Bingham Yield Stress (Pa)	Casson Yield Stress (Pa)	Slotted Plate Yield Stress (Pa)
Trial 1	0.007	0.123	0.050
Trial 2	0.020	0.203	0.053
Trial 3	0.014	0.084	N/A
Trial 4	0.006	0.017	0.054
Average	0.012	0.107	0.052
Average Percent Error (%)	17.11	12.72	2.970

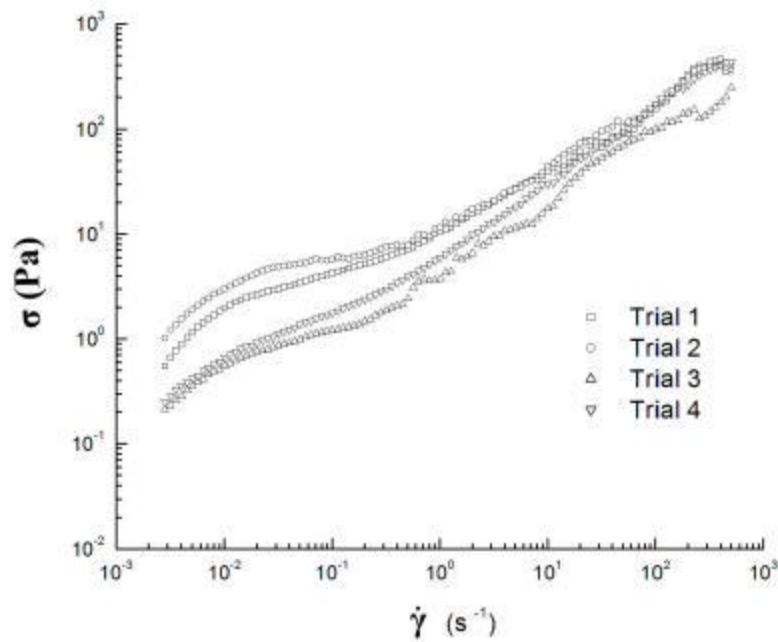


Figure 9
Sample CSS-1 results

Sample CRS – 2P. The data obtained for the sample CRS-2P via the rotational measurements are shown in figure 10. The computed Casson and Bingham yield stress values are shown in table 12, along with the slotted plate results. Again, the extrapolations used the data at the lower values of shear rate, resulting in major differences from the slotted plate experimental results.

Table 12
Sample CRS-2P results

	Bingham Yield Stress (Pa)	Casson Yield Stress (Pa)	Slotted Plate Yield Stress (Pa)
Trial 1	$4.0 \cdot 10^{-5}$	$1.76 \cdot 10^{-07}$	0.031
Trial 2	$3.0 \cdot 10^{-7}$	$1.00 \cdot 10^{-08}$	0.033
Trial 3	$3.0 \cdot 10^{-8}$	$4.00 \cdot 10^{-12}$	0.037
Average	$1.34 \cdot 10^{-5}$	$6.21 \cdot 10^{-08}$	0.034
Average Percent Error (%)	81.63	73.39	3.28

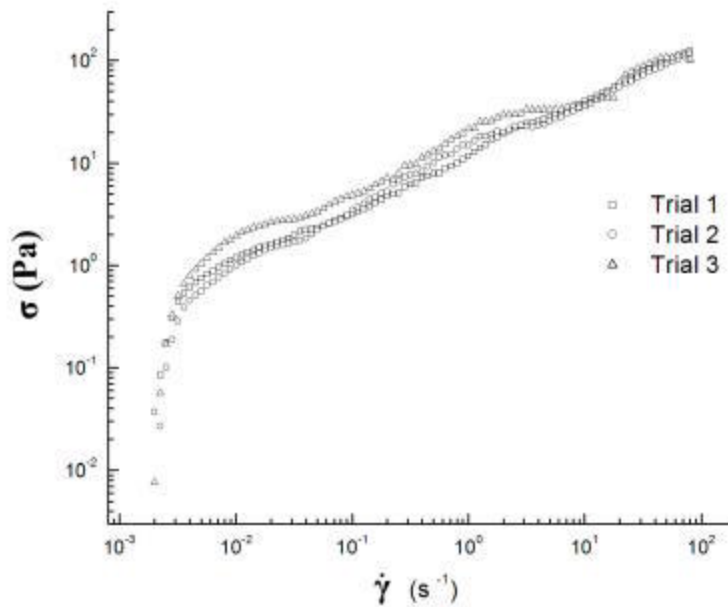


Figure 10
Sample CRS-2P results

Sample AE-P. The data obtained for the sample AE-P via the rotational measurements are shown in figure 11. The computed Casson and Bingham yield stress values are shown in table 13, along with the slotted plate results. Again, the extrapolations used the data at the lower values of shear rate.

Table 13
Sample AE-P results

	Bingham Yield Stress (Pa)	Casson Yield Stress (Pa)	Slotted Plate Yield Stress (Pa)
Trial 1	$6.00 \cdot 10^{-07}$	$1.3 \cdot 10^{-3}$	0.0015
Trial 2	$1.00 \cdot 10^{-08}$	$3.4 \cdot 10^{-4}$	0.0017
Trial 3	$6.00 \cdot 10^{-03}$	$7.5 \cdot 10^{-2}$	0.0016
Average	$2.00 \cdot 10^{-03}$	$2.5 \cdot 10^{-2}$	0.0016
Average Percent Error (%)	83.31	83.27	2.09

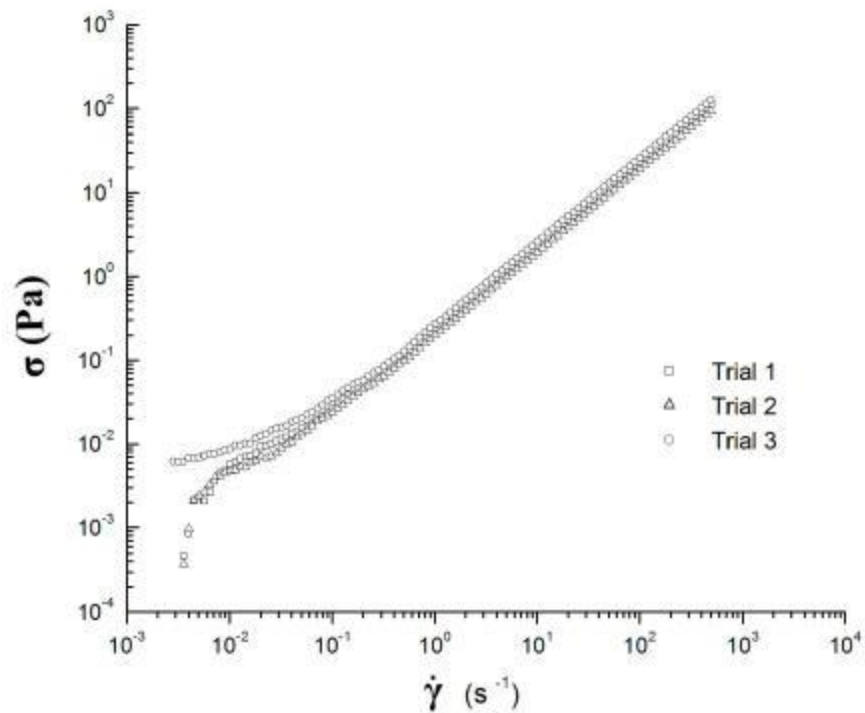


Figure 11
Sample AE-P results

Table 14
Bohlin Visco 88 viscometer results

Trial	SS-1		CRS-2		Slotted Plate (Pa)	
	Bingham (Pa)	Casson (Pa)	Bingham (Pa)	Casson (Pa)	SS-1	CRS-2
1	0.64	0.049	0.029	0.002	0.012	0.035
2	0.58	0.047	0.47	0.009	0.010	0.034
3	0.59	0.052	0.77	0.03	0.011	0.035
Average	0.60	0.049	0.42	0.014	0.011	0.035
Average Percent Error (%)	2.95	0.34	87.2	74.5	2.51	1.95

Trial	AES-300		CSS-1		Slotted Plate (Pa)	
	Bingham (Pa)	Casson (Pa)	Bingham (Pa)	Casson (Pa)	AES-300	CSS-1
1	3.577	1.283	0.0255	0.0005	0.204	0.050
2	4.127	1.239	0.112	0.00125	0.201	0.053
3	3.494	1.239	0.0501	2.5*10 ⁻⁶	0.209	0.054
Average	3.733	1.254	0.0625	0.006	0.205	0.052
Average Percent Error (%)	3.48	0.78	27.15	47.74	0.705	2.970

Trial	CRS-2P		AE-P		Slotted Plate (Pa)	
	Bingham (Pa)	Casson (Pa)	Bingham (Pa)	Casson (Pa)	CRS-2P	AE-P
1	0.268	0.0395	0.2874	0.0095	0.031	0.0015
2	0.131	0.0016	0.2697	0.00897	0.033	0.0017
3	0.922	0.057	N/A	N/A	0.037	0.0016
Average	0.440	0.0327	0.279	0.009	0.034	0.0016
Average Percent Error (%)	37.99	42.39	1.59	1.44	3.28	2.09

Yield Stress Results Obtained with Bohlin 88 Viscometer

The data in table 14 show the yield stress results for all 6 samples obtained with a concentric cylinder geometry used with the Bohlin 88 instrument. This instrument generated data equivalent to data obtained with a Brookfield viscometer.

The Bingham yield stress result was obtained via extrapolation of the $t - \dot{\gamma}$ data (see figure 12) to zero shear rate. Similarly, the Casson yield stress result was obtained via extrapolation of the data as shown in figure 13.

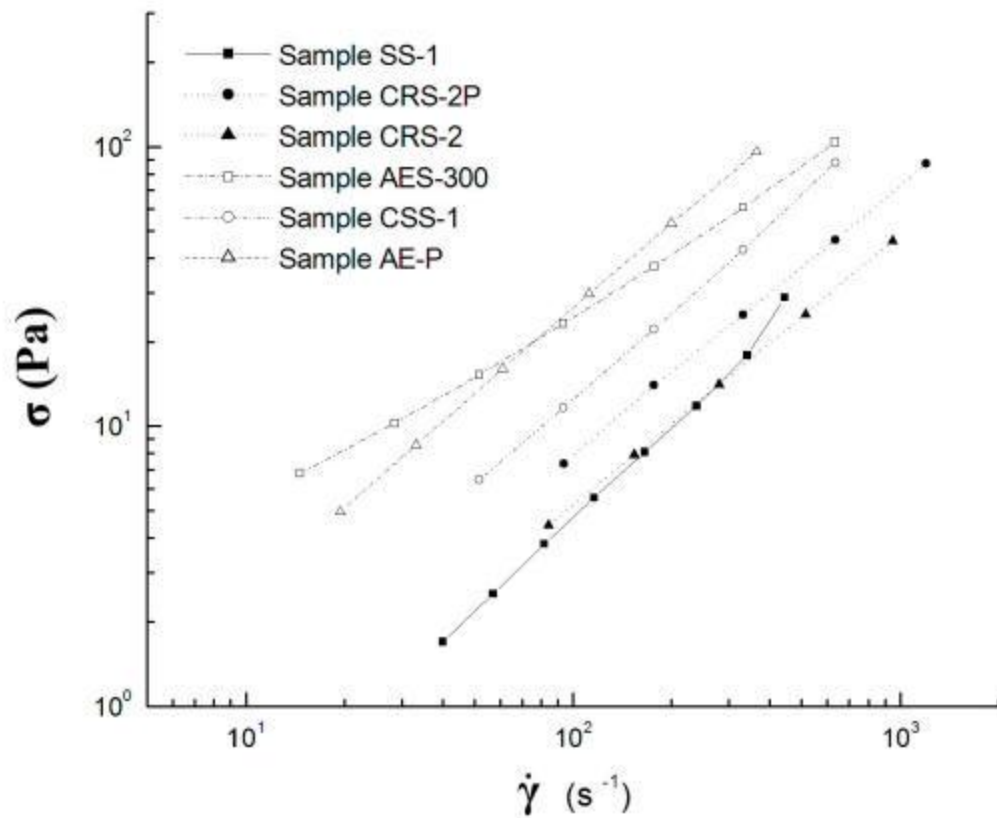


Figure 12
Bingham model curve fit

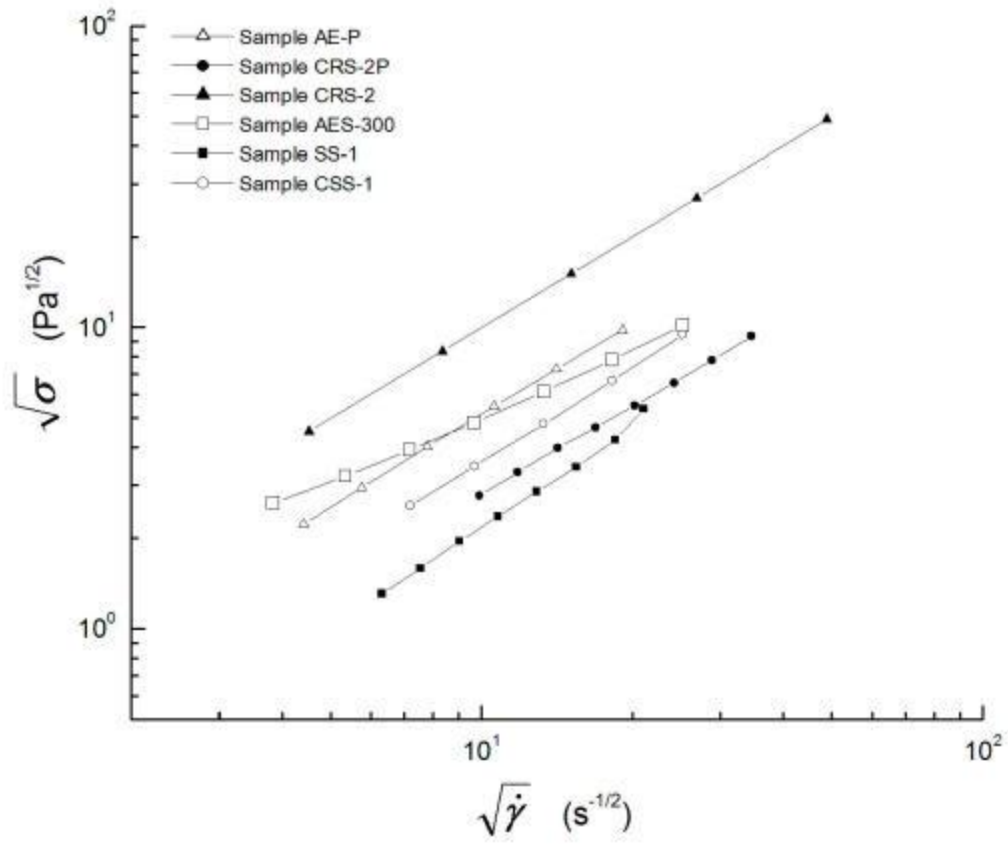


Figure 13
Casson model curve fit

Discussion of Data Obtained via Rotational Rheometers.

The yield stress of asphalt emulsions is difficult to measure with any degree of certainty using the cone and plate or parallel plate geometries. Although the TA AR-2000 rheometer is a top-of-the line research instrument, it is not sensitive enough at the very low shear rate region to produce reproducible data for the shear stress–shear rate relationships, from which the yield stress is obtained via extrapolation. The underlying assumption of the Bingham model is Newtonian behavior of the sample in the flow region. The data prove that the asphalt emulsions do not behave as Newtonian fluids in the low shear rate region. The extrapolation to zero shear rate thus gives inaccurate results.

Table 15
Summary of the results for rotational rheometers and comparison with the slotted plate results

	SS-1	CRS-2	CRS-2P	AES-300	AE-P	CSS-1
TA AR-2000 Results						
Bingham Yield Stress (Pa)	0.117	0.243	$1.34 \cdot 10^{-05}$	0.433	$2.00 \cdot 10^{-03}$	0.012
Casson Yield Stress (Pa)	0.029	0.139	$6.21 \cdot 10^{-08}$	0.079	$2.50 \cdot 10^{-02}$	0.107
Bohlin 88 Results						
Bingham Yield Stress (Pa)	0.60	0.42	0.440	3.733	0.279	0.0625
Casson Yield Stress (Pa)	0.049	0.014	0.0327	1.254	0.009	0.006
Slotted Plate Yield Stress (Pa)	0.011	0.035	0.034	0.205	0.0016	0.0525

The TA AR-2000 advanced rheometer achieved shear rate values as low as 10^{-3} s^{-1} , which provided more confidence in the results obtained via extrapolation. However, even with data at such low shear rate values, the results were inconsistent for the most part. At first sight, one can conclude that the Casson model is better at predicting the yield stress of the asphalt emulsions. At higher shear rates, all of the samples exhibited power law behavior, and at very high shear rates, they exhibited Newtonian behavior, as expected. The curves converged for the shear rate values greater than 10 s^{-1} . The Casson and Bingham models overestimated the true yield stress of the material.

Because the Bohlin Visco 88 viscometer is incapable of attaining low shear rates values

(< 10^0 s^{-1}), it compounds the errors resulting from the extrapolation of the data to the lower shear rate regions. The results of the Bohlin 88 tests are given in table 15. These results indicate that using rotational viscometers at higher shear rates generates reproducible results, but the extrapolations to zero shear rate are highly dependent on the model (Bingham, Casson, etc.) used. Yield stress determinations using rotational geometries followed by extrapolation procedures should be avoided.

Saybolt Viscosity Determination of Asphalt Emulsions

Procedure

The sample was prepared according to the AASHTO T72-97 standard procedure. The water bath for the Saybolt apparatus was established at 25°C, and the sample was preheated to 25°C. The sample was hand stirred and then strained, using number 100 wire cloth in the filter funnel, directly into the viscometer until the level was above the overflow rim. The efflux time was measured using a RadioShack Multifunction LCD Stopwatch to the nearest 0.1 s.

Results

Saybolt testing was performed on the four samples following the AASHTO T 72-97 standard at 25°C using water as a bath medium. The shortage of samples prevented more tests at higher temperatures.

Discussion of Saybolt Measurement Results

The Saybolt viscosity, given in units of (s), is not comparable to the proper viscosity that relates shear stress to shear rate and is expressed in $(Pa \cdot s)$. Note that the viscosity of a complex system, such as an asphalt emulsion, is a function of shear rate. Because we are dealing with a non-Newtonian viscosity, using a “one point viscosity value” as a quality control tool cannot be justified.

The idea of using a single value quality control parameter is appealing. The results of this preliminary research program suggest that the sample yield stress is a good candidate for such a one point measure, as it can be determined within an acceptable error margin. In addition, the concept of a yield stress provides a solid physical basis for this choice of quality control.

Table 16
Saybolt results

Sample	Trial	Efflux Time	Correction Factor	"Viscosity"
CSS-1	1	47.84	1.0546	50.45
	2	55.75	1.0572	58.94
	3	59.28	1.0572	93.19
Average				67.53
AES-300	1	96.43	1.0546	101.70
	2	102.91	1.0546	108.53
	3	112.28	1.0572	118.70
	4	101.3	1.0572	107.09
				111.44
SS-1	1	23.22	1.0572	24.55
	2	23.69	1.0572	25.05
	3	20.5	1.0546	21.6193
	4	25.28	1.0546	26.66
				24.44
AE-P	1	88.5	1.0572	93.56
	2	92.35	1.0572	97.63
	3	92.75	1.0546	97.81
	4	99.69	1.0546	105.13
				100.19
CRS-2	1	525.5	1.0572	555.56
	2	530.7	1.0572	561.06
	3	527.6	1.0546	556.41
	4	535.0	1.0546	564.21
				559.31
CRS-2P	1	620.1	1.0572	655.57
	2	618.2	1.0572	653.56
	3	625.9	1.0546	660.07
	4	627.3	1.0546	661.55
				657.69

CONCLUSIONS

To our knowledge, no yield stress measurements have been reported for asphalt emulsions. In fact, little attention has been given to any material with low yield stress values [15]. Measuring such low values of yield stress is difficult using traditional methods. The slotted-plate technique accurately determined the yield stress of these emulsions. Other accepted standard tests were performed for comparison. Yield stress measurements obtained via extrapolation of shear stress-shear rate data are definitely not reliable. Another disadvantage of the standard (extrapolation) testing methods is the fact that the yield stress determinations also rely on the choice of a rheological model.

The Saybolt test provides a single viscosity value for a given temperature; however, the emulsions are not Newtonian fluids at lower temperatures. In addition the Saybolt viscosity does not have the units of viscosity, so a viscosity function (curve) is required to express the sample viscosity. Determining a single viscosity point for a non-Newtonian material does not characterize the material. On the other hand, the static yield stress for a particular material is a constant. Thus, this static yield stress determination is preferable as a quality control parameter for asphalt emulsions, provided its value can be obtained within an acceptable magnitude of error.

The purpose of this project was to begin comparing several techniques for determining the yield stress of asphalt emulsions. The project also tested the ability of the slotted plate technique to determine of the yield stress values of asphalt emulsions. Six samples of asphalt emulsions were characterized using concentric cylinders, parallel plate and cone and plate geometries (i.e. rotational rheometers), a slotted plate technique, and a Saybolt viscometer. Results show that the slotted plate technique is superior (i.e. no extrapolation is involved) to the rotational rheometers because it is a direct measurement technique that measures the yield stress in undisturbed samples by carefully inserting the plate in the sample and allowing the sample to come to equilibrium. The slotted plate yield stress results were consistent.

The rotational rheometers did not allow for a direct measurement of the yield stress, as extrapolation of rheometric data was required. The yield stress values obtained via the Casson model were comparable to the slotted plate technique results. The Bingham model did not always predict the yield stress accurately.

The Bingham and Casson yield stresses were determined using a select range of shear rates (lowest possible) from the data obtained with the TA-AR 2000 rheometer. As mentioned earlier, the data were inconsistent at shear rates below 1 s^{-1} .

The Saybolt testing was performed following the AASHTO T 72-97 standard at 25°C. The results from Saybolt testing are not directly comparable to the yield stress results because the Saybolt viscosity is a measure of the time required for 60 ml of emulsion to flow through a capillary, whereas the yield stress is a measure of the stress necessary to induce the flow in the material. However, both of those values are appealing since they are single point characterization parameters. While a single point characterization is practical, such a characterization must be based on solid scientific principles. This is not the case for the Saybolt measurement since the $h - \dot{g}$ relationship is not considered.

The static yield stress determined via the slotted plate technique was a constant. Consistent results within 6 percent error were obtained. The slotted plate technique deserves further investigation involving an expanded array of industrially important emulsions to determine the effects of asphaltene interactions and emulsifying agents on the yield stress. Other variables of interest include the thermal dependence of the yield stress as well as Oswald ripening effects. The ultimate goal of such research would be to establish a new standard procedure to characterize asphalt emulsions.

From a rheological standpoint, the yield stress grading is preferable to the other techniques described in this report. Until now determining the precise yield stress value of the emulsions of interest was nearly impossible, since the yield stress is of a rather small magnitude. Current results suggest that with the slotted plate technique, the static yield stress of asphalt emulsions can be determined with confidence.

NOTATION

Ca	Capillary Number
D_v	vane diameter (m)
F	orifice calibration constant
F_i	“Initial force” (Pa)
F	force at time t_r (Pa)
h	gap between two plates (m)
H	vane height (m)
M	viscosity ratio of the dispersed to the suspending fluids
r	radial position
R	radius of the cone (m)
R	radius of the vane (m)
t	efflux time (s)
t_r	time at which flow is initiated (s)
T	torque (N·m)
T_m	maximum torque (N·m)
S	plate surface area (m ²)
z	axial position

Greek Letters

f	volume fraction
u	saybolt “viscosity” (SFS)
q_0	cone angle (rad or deg)
$\dot{\underline{\underline{g}}}$	rate of deformation tensor $\{ = \underline{\nabla}v + (\underline{\nabla}v)^+ \}$
$\dot{\underline{\underline{g}}}_{rz}, \dot{\underline{\underline{g}}}_{qf}, \dot{\underline{\underline{g}}}_{yx}$	shear rate (s ⁻¹)
$\dot{\underline{\underline{g}}}_R$	wall-shear rate in Poiseuille flow (s ⁻¹)
$\underline{\underline{s}}_{rq}$	(r -?) component of shear stress tensor $\underline{\underline{s}}$
$\underline{\underline{s}}$	stress tensor
$\underline{\underline{s}}_0$	yield stress (Pa)
$\underline{\underline{s}}_e$	end surface shear stress (Pa)
$\underline{\underline{s}}_w$	wall shear stress $\{ = \underline{\underline{s}}_{rq} _{r=R_v} \}$ (Pa)
$\underline{\underline{s}}_{xy}, \underline{\underline{s}}_{qf}$	shear stress (Pa)
Γ	surface tension of the solvent (N·m ⁻¹)
Ω	angular velocity (rad/s)
η	viscosity of the suspension (Pa·s)
h_0	Newtonian viscosity (constant) (Pa·s)
h_r	relative viscosity (Pa·s)
h_s	viscosity of the solvent (Pa·s)

REFERENCES

1. Carreau, P., De Kee, D. and Chhabra, R., *Rheology of Polymeric Systems*. Hanser, New York, 1997.
2. Larson, R., *The Structure and Rheology of Complex Fluids*. Oxford University Press, New York, 1999.
3. Goto, H. and Kuno, H. "Flow of Suspensions COntaining Particles of Two Different Sizes Through a Capillary Tube." *Journal of Rheology*, Vol. 36, No. 5, 1982, 387-398.
4. Hoffman, R. "Factors Affecting The Viscosity of Unimodal And Multimodal Colloidal Dispersions." *Journal of Rheology*, Vol. 36, No. 5, 1992, 947-964.
5. Van Der Werff, J. C. and De Kruff, C. G. "Hard-Sphere Colloidal Dispersions: The Scaling of Rheological Properties With Particle Size, Volume Fraction, and Shear Rate." *Journal of Rheology*, Vol. 33, No. 3, 1989, 421-454.
6. Zhu, L., "A Slotted Plate Device to Measure Yield Stress," PhD dissertation, Tulane University, New Orleans, 2001.
7. The Surfactants Virtual Library, March 26, 2003, <http://www.surfactants.net/emulsion.htm>.
8. AEMA, Asphalt Emulsion Manufacturers Association. Frequently Asked Questions, N.d., June, 9, 2003, <http://www.aema.org/FAQ.htm>.
9. Kenedy, W. T. and Cominsky, J. R., "Hypothesis and Models Employed in the SHRP Asphalt Research Program." Strategic Highway Research Program, Washington D.C., 1990.
10. Bahia, H. U., Hanson, D. I., Zeng, M., Zhai, H., Khatri, M. A. and Anderson, R. M., "Characterization of Modified Asphalt Binders in Superpave Mix Design," NCHRP Report 459, National Academy Press, Washington, D.C., 2001.
11. Deshpande P, V. S., Shahanawaz A. and M.V. Arum, "Microstructure Related Rheological Behavior of Asphalt,," Indian Institute of Technology, Madras, Chennai, India, 2003.

12. Asphalt Emulsions, Ergon, Inc., June, 9, 2003,
http://www.ergon.com/html/asphalt_emulsions.html.
13. Koch Pavement Solutions, Koch Material Company, June, 9, 2003,
<http://www.kochpavementsolutions.com/Solutions/emulsions.htm>.
14. Nguen, D. Q. and Boger, D. V. "Yield Stress Measurement for Concentrated Suspensions." *Journal of Rheology*, Vol. 27, No. 4, 1983, 321-349.
15. Zhu, L., Sun, N., Papadopoulos, K. and De Kee, D. "A Slotted Plate Device for Measuring Static Yield Stress." *Journal of Rheology*, Vol. 45, No. 5, 2001, 1105-1122.

Performance-Related Test for Asphalt Emulsions

by

Daniel De Kee, Ph.D.
Professor of Chemical and Biomolecular Engineering
Director, Tulane Institute for Macromolecular Engineering and Science (TIMES)

Christopher David Abadie, P.E.
LTRC

Max Hetzer
Graduate Research Assistant

Kyle Frederic
Undergraduate Research Assistant

LTRC Project No. 03-7B
State Project No. 736-99-1142

conducted for

Louisiana Department of Transportation and Development
Louisiana Transportation Research Center

The contents of this report reflect the views of the author/principal investigator who is responsible for the facts and the accuracy of the data presented herein. The contents do not necessarily reflect the views or policies of the Louisiana Department of Transportation and Development or the Louisiana Transportation Research Center. This report does not constitute a standard, specification, or regulation.

October 2004

ABSTRACT

Yield stress was investigated as a potential quality control parameter for asphalt emulsions. Viscometric data were determined using the concentric cylinder, parallel plate, and cone and plate geometries with rotational rheometers. We also investigated the use of a novel slotted plate technique to determine the yield stress in a direct way—that is to say, without extrapolation. The Saybolt “viscosity” was determined with a Saybolt Viscometer following the AASHTO T 72-97 standard procedure. The slotted plate technique generated reproducible and consistent results that were far superior to those obtained by rotational rheometer techniques. The yield stress of the emulsions appears to be a more accurate measure of the performance specification for asphalt emulsions than the Saybolt “viscosity” data.

IMPLEMENTATION STATEMENT

Currently, the Saybolt test is used for quality control analysis of asphalt emulsions. With the Saybolt test procedure, the time required for 60 milliliters of a test fluid to flow through a calibrated orifice is measured. This time measurement is then associated with viscosity of the material. This procedure is reliable only when the material in question is Newtonian; the viscosity of the material is shear rate independent. The asphalt emulsions were proved to be non-Newtonian materials. The current standard Saybolt test procedure is not reliable since the shear rate that the material experiences during the test changes due to a continuously changing hydrostatic head. However, the Saybolt test procedure produces a one-point quality control parameter, which is an attractive alternative to rheological characterization involving dozens of test points.

The yield stress of multiphase materials such as asphalt emulsions is a one-point characterization parameter of the flow properties of multiphase materials. Previously, accurately determining the yield stress of materials such as asphalt emulsions was nearly impossible because of the technique involving extrapolation of viscometric data to zero shear rate. The slotted plate technique developed at Tulane University can provide accurate and reliable yield stress values of asphalt emulsions.

This report presents the results of a preliminary study to determine the feasibility of using the slotted plate technique to accurately determine the yield stress of select asphalt emulsions. The results of this study should lead to a more extensive research project that would develop a new standard quality control test for asphalt emulsions.

TABLE OF CONTENTS

ABSTRACT.....	v
IMPLEMENTATION STATEMENT	vii
TABLE OF CONTENTS.....	ix
LIST OF TABLES	xi
LIST OF FIGURES	xiii
INTRODUCTION.....	1
Background	2
Emulsions.....	3
OBJECTIVE.....	5
SCOPE.....	7
METHODOLOGY	9
Saybolt and Capillary Viscometry.....	9
Rheometers.....	11
Bohlin Visco 88 Viscometer	11
Rotational Viscometers (TA Advanced Rheometer).....	11
Models for Materials that Exhibit a Yield Stress	13
Direct Yield Stress Measuring Devices	15
Vane Technique	15
Slotted Plate Technique.....	15
RESULTS AND DISCUSSION	19
Yield Stress Testing Using A New Slotted Plate Apparatus	19
Procedure.....	19
Sample SS-1	19
Sample CRS-2	20
Sample AES-300.....	21
Sample CSS-1.....	21

Sample CRS-2P.....	22
Sample AE-P.....	22
Analysis and Discussion of Slotted Plate Technique Results	23
Yield Stress Results Using Rotational Rheometers.....	24
Procedure.....	24
Results Obtained with TA AR-2000 Rheometer	25
Yield Stress Results Obtained with Bohlin 88 Viscometer.....	33
Discussion of Data Obtained via Rotational Rheometers.....	35
Saybolt Viscosity Determination of Asphalt Emulsions	36
Procedure.....	36
Results.....	36
Discussion of Saybolt Measurement Results.....	36
CONCLUSIONS	39
NOTATION	41
Greek Letters.....	41
REFERENCES	43

LIST OF TABLES

Table 1 Sample SS-1 results	20
Table 2 Sample CRS-2 results	21
Table 3 Sample AES-300 results.....	21
Table 4 Sample CSS-1 results.....	22
Table 5 Sample CRS-2P results	22
Table 6 Sample AE-P results.....	23
Table 7 Yield stress values for all samples.....	23
Table 8 Sample SS-1 results	25
Table 9 Sample CRS-2 results	26
Table 10 Sample AES-300 results.....	28
Table 11 Sample CSS-1 results.....	29
Table 12 Sample CRS-2P results	30
Table 13 Sample AE-P results.....	31
Table 14 Bohlin Visco 88 viscometer results	32
Table 15 Summary of the results for rotational rheometers and comparison with the slotted plate results.....	35
Table 16 Saybolt results	37

LIST OF FIGURES

Figure 1 Sample CRS-2P under 40X magnification.....	4
Figure 2 Saybolt viscometer	10
Figure 3 Kinematic viscometers	10
Figure 4 Slotted plate set up	16
Figure 5 Force - time curve	17
Figure 6 Sample SS-1 results	26
Figure 7 Sample CRS-2 results	27
Figure 8 Sample AES-300 results.....	28
Figure 9 Sample CSS-1 results.....	29
Figure 10 Sample CRS-2P results.....	30
Figure 11 Sample AE-P results.....	31
Figure 12 Bingham model curve fit.....	33
Figure 13 Casson model curve fit.....	34

INTRODUCTION

The rheology of suspensions and emulsions is of great interest to the industrial community since many processes involve “particles” of some kind. However, the rheological analysis of such systems is a difficult topic. The earlier models that are available to describe the rheological behavior of suspensions apply only to very dilute suspensions. Einstein’s model [1], for example, assumes a dilute suspension of rigid spheres in a Newtonian fluid, and can predict rheological behavior of suspensions only for limited cases. Einstein’s relation is given by

$$\mathbf{h}_r = \frac{\mathbf{h}}{\mathbf{h}_s} = 1 + \frac{5}{2} \mathbf{f} \quad (1)$$

where \mathbf{h}_r is the relative viscosity, \mathbf{h} is the viscosity of the suspension, \mathbf{h}_s is the solvent viscosity, and \mathbf{f} is a volume fraction occupied by the spheres. Einstein’s theoretical result is only valid for very low concentrations ($\mathbf{f} < 0.01$).

Larson [2] considers the simplest case of a steady flow of a dilute suspension of Newtonian drops or bubbles in a Newtonian medium through a capillary. If the capillary number,

$$Ca = \mathbf{h}_s \dot{\mathbf{g}}_{rz} a / \Gamma \quad (2)$$

with (a) being the surface area and (Γ) the surface tension of the solvent, is small, the drops or bubbles do not deform under flow and the suspension viscosity at a steady state is given by Taylor’s extension of the Einstein formula for solid spheres:

$$\mathbf{h}_r \equiv \frac{\mathbf{h}}{\mathbf{h}_s} = 1 + \frac{1 + \frac{5}{2} M}{1 + M} \mathbf{f} \quad (3)$$

where M is the ratio of the viscosities of the dispersed to the suspending fluids. As $M \rightarrow \infty$, the droplets behave like hard spheres, and Einstein’s result is recovered. As $M \rightarrow 0$, the relative viscosity is lower, $\mathbf{h}_r = 1 + \mathbf{f}$, which is generally true for bubbles. The viscosity of a suspension of bubbles is less than that of a suspension of hard spheres at a given volume fraction because liquid

bounding the surface of a bubble can flow. Hence, bubbles disturb the flow field of the external fluid less than do hard spheres [2].

Some researchers found that the viscosity of suspensions containing two types of solid particles exhibit a decrease in viscosity [3, 4]. Goto and Kuno determined that the relative viscosity of the suspension of a single component was lowered by mixing particles of different sizes [3]. The relative apparent viscosity of the suspension was at a minimum when the volume fraction for the larger particles with respect to the total solids was about 60 percent. Also, the possible lubrication effect by small particles was observed. Hoffman observed that as the size of the particles in the suspension decreased, the viscosity of the suspension rose exponentially as the number of particles increased [4]. The suspension became strongly shear thinning for $f > 0.35$; Van Der Werff and De Kruif, showed similar behavior for four submicron sterically stabilized silica dispersions with differing particle sizes [5]. They found that the high and low shear limiting viscosities are functions of the volume fraction only, and the volume fraction at which the viscosity diverges is independent of the particle size. Note that asphalt emulsions are dispersions of droplets with a wide size distribution.

We investigated the use of the yield stress value to characterize asphalt emulsions and to possibly replace the Saybolt grading procedure with the emulsion yield stress, which should be a more accurate quality control tool. Materials such as suspensions, coatings, and emulsions possess a three-dimensional microstructure, which imparts solid-like properties but is susceptible to structural breakdown under an applied force [1]. The flow properties of these materials are between those of a solid and a liquid. When the material is subjected to a small stress, it behaves as a solid. However, when this stress is large enough, the sample behaves as a liquid and begins to flow. Ketchup is a well known example of a yield stress material (yield stress value is 15 Pa for Heinz 57 ketchup). If the ketchup bottle is turned over, the ketchup will not flow until sufficient force is applied. Yield stress is defined as the minimum amount of force that must be applied to degrade a material's structure and induce flow. It is important that any multiphase material of industrial significance be accurately characterized by this critical control parameter, as the yield stress can play an important role in determining the processing constraints during production, storage, transportation, and overall performance of the product [6].

Background

Emulsions

An emulsion is defined as a stable dispersion of one liquid in a second immiscible liquid [7].

Furthermore, an asphalt emulsion is a combination of three main substances: asphalt, water, and a small amount of an emulsifying agent or “soap” that stabilizes the emulsion [8]. One of the asphalt models has been proposed by Kennedy and Cominsky [9], who considered an asphalt emulsion as a suspension of aromatic, high-molecular weight, core molecules dispersed in a medium of relatively low-molecular weight molecules. The dispersed phase is viewed as being peptized by absorbed aromatic molecules lower in molecular weight than the core materials, which are soluble in the dispersing medium. The core materials are considered to be asphaltene micelles, the peptizing agents are considered to be resins, and the dispersing media are considered to be oils (maltenes).

Kennedy and Cominsky’s [9] working hypothesis of the asphalt structure states that the phase consisting of relatively aliphatic, non-polar molecules that are low in heteroatoms disperses the micellar structures of asphaltene-like molecules. These asphaltene-like molecules are aromatic, polar, and contain heteroatom functional groups. The size of the micelles may vary widely, but for emulsion CRS-2P the largest droplet size was 95 μm , and the average droplet size was 65 μm . Some asphalt emulsions have an observable amount of micellar structures that are small in size and number, are well dispersed, and exhibit Newtonian behavior [10]. Other asphalt emulsions contain substantial amounts of poorly dispersed large micelles and are capable of forming three-dimensional networks of asphaltene micelles within the emulsion, thus exhibiting non-Newtonian behavior [10].

The four most important components of asphalt are oil, crystallizable waxes, resin, and asphaltenes. The oil fraction of asphalt includes structures of fused naphthenic rings with linear and branched aliphatic side chains of various lengths. The resin fraction of asphalt consists of hundreds of different hydrocarbons, but the general nature of resin fraction consists of polycyclic molecules containing saturated aromatic, heteroaromatic rings and heteroatoms in various functional groups [11].

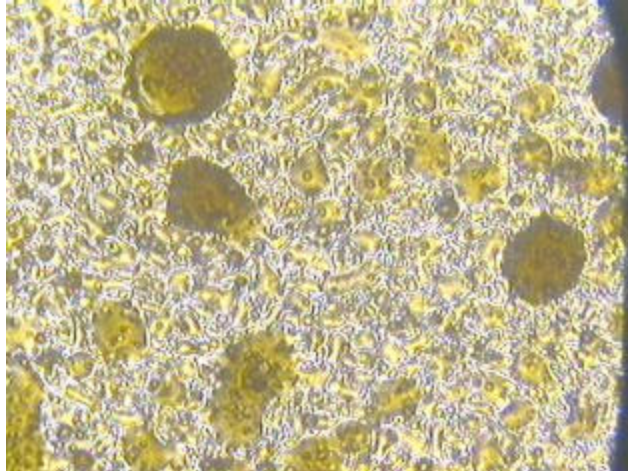


Figure 1
Sample CRS-2P under 40X magnification, 1 cm = 100 μ m

These components are sheared in a high-speed mixer called a colloid mill that produces tiny asphalt droplets. The emulsifier, which is a surface-active agent, keeps the asphalt droplets in a stable emulsion. The result is a liquid product with a consistency ranging from that of milk to heavy cream, which can be used in cold processes for road construction and maintenance.

Asphalt emulsions can be classified into three categories that refer to the electrical charges surrounding the asphalt particles: anionic, cationic, or nonionic. They are further classified on the basis of how quickly they coalesce; that is, how quickly they form asphalt cement [8].

Many advantages result from using asphalt emulsions. Asphalt emulsions do not require a petroleum solvent to liquefy, and they can usually be used without applying additional heat. Both of these factors contribute to energy savings. Additionally, asphalt emulsions are environmentally friendly. Hardly any hydrocarbon emissions are created by their use [8]. Because of their environmental properties, energy efficiency, and cost effectiveness, emulsions will likely emerge as the asphalt product of the future for pavement maintenance, roofing, and specialty industrial applications [8, 12]. Choosing the right emulsion and application technique yields substantial economic and environmental benefits [13].

OBJECTIVE

This initial research project characterized several different samples of asphalt emulsions and compared the results from different types of rheological tests. Several testing procedures were used for this project to reveal some rheological characteristics of the emulsions. The novel slotted-plate technique, measurements using coaxial cylinder geometry (Bohlin Visco 88 rheometer), Saybolt viscometer testing, as well as cone and plate and parallel plate geometries (TA AR2000 rheometer) were performed to identify the sample yield stress and viscosity functions.

SCOPE

Six samples of asphalt emulsions provided by LTRC were tested with the slotted plate technique at 25°C. The 2ⁿ factorial test design was used to determine the effects of several variables on the yield stress of emulsions. The maximum test time was optimized to be less than 30 minutes in order to be comparable to the Saybolt test procedure.

The viscometric data was determined with the TA AR-2000 rheometer and Bohlin Visco 88 viscometer. The data was fitted to Bingham and Casson models to determine the yield stress value of the emulsion samples. The temperature was kept constant at 25°C, and the sample preparation procedure was same as for the slotted plate technique.

The Saybolt data was obtained at the LDOT 2 Lab, using the AASHTO T 72-94 standard procedure. The data was analyzed with MS Excel and then used to determine the quality of the asphalt emulsions samples.

METHODOLOGY

Saybolt and Capillary Viscometry

Rheological properties, such as viscosity, are measured via rheometers such as the Bohlin Visco 88 rotational viscometer, the Saybolt viscometer, and/or the TA AR-2000 advanced rheometer. One can obtain qualitative information about the flow characteristics of a Newtonian fluid by measuring the time required for a fixed volume of a fluid (at a given temperature) to flow through a calibrated orifice or capillary tube. Note that such a measurement is not associated with viscosity units, which are $Pa \cdot s$ in SI units. Several types of viscometers are used today. The Saybolt viscometer shown in figure 2 is used to determine the viscosity of Newtonian fluids. It consists of four cylinders (sample holders) of equal volume with capillary outlet tubes at the bottom of the cylinders. The cylinders are immersed in a constant temperature bath. The sample is loaded in the cylinders and allowed to reach thermal equilibrium. Then the fluid is allowed to flow through an orifice (capillary) and the efflux time, which is the time required for 60 milliliters of fluid to flow through the capillary, is recorded.

The sample is stirred by a mixer prior to a measurement to achieve a similar initial structure and generate reproducible results. The time measured is used to express the fluid's viscosity in Saybolt Universal Seconds or Saybolt Furol Seconds. (Note: the asphalt emulsions are always measured in Saybolt Furol Seconds.)

$$\mathbf{n} = Ft \tag{4}$$

Where \mathbf{n} is the kinematic viscosity of the fluid expressed in seconds, F is the calibration constant of the orifice (capillary), and t is the efflux time. The calibration constant is determined for each orifice using a standard with a known viscosity.

The glass capillary viscometers, shown in figure 3, are examples of a second type of viscometer. These viscometers are used to measure kinematic viscosity. Like the Saybolt viscometer, a glass capillary is used to measure the time in seconds required for the test fluid to flow through a bulb. This time is multiplied by a temperature constant, determined from the calibration of the tube in use, to provide the viscosity expressed in centistokes.



Figure 2
Saybolt Viscometer

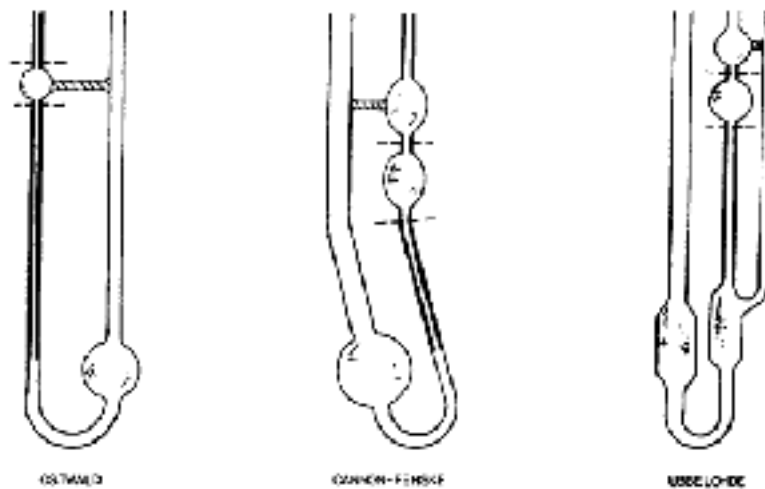


Figure 3
Kinematic Viscometers

Rheometers

Bohlin Visco 88 Viscometer

The portable and easy-to-use Bohlin Visco 88 viscometer uses coaxial cylinder geometry. In this study, the sample was prepared the same way as a Saybolt test sample. The sample was loaded until the thermocouple was slightly immersed. A range of shear rates was chosen, and shear stress versus shear rate data was plotted; the yield stress was determined with an extrapolation procedure from the obtained viscometric data.

Coaxial Cylinder Geometry. Most modern rheometers are rotating devices that can rapidly determine the viscosity curve as well as other important rheological material functions. Commercial rheometers are available with computer control and software packages for data analysis. The measurements are made using three possible geometries: coaxial cylinders, cone and plate, and parallel plates. Coaxial cylinders were the first rotating devices used to measure viscosity. Basically, the geometry consists of a stationary cylinder and a rotating cylinder. The sample is loaded in the gap between the cylinders, which should be small to approximate a constant shear rate. Depending on the setup, either the inner or outer cylinder rotates. After the torque is measured, the viscosity can then be calculated [1].

Rotational Viscometers (TA Advanced Rheometer)

The TA AR2000 advanced rheometer is a powerful and versatile research-grade rheometer. This instrument utilizes different measuring system geometries than used with the Bohlin 88 viscometer. Parallel-plate and cone and plate geometries are used.

Cone and Plate Geometry. The cone and plate geometry is the most popular for determining the viscosity of viscoelastic fluids. A small sample is placed in the space between a plate of radius R and a cone of the same radius with a very small angle, so that the shear rate is constant in the gap. The sample should have a free spherical-shaped surface at the outer edge. For viscous fluids, the cone can be positioned below the plate, and either the cone or the plate can be rotated. The shear stress can be determined from the measured torque as follows:

$$T = 2\mathbf{p} \int_0^R \mathbf{s}_{qf} r^2 dr = \frac{2}{3} \mathbf{p} R^3 \mathbf{s}_{qf}$$

(5)

where T is the torque, \mathbf{s}_{qf} is the shear stress, and $\dot{\mathbf{g}}_{qf}$ is the shear rate

From

$$\mathbf{s}_{qf} = -\mathbf{h}\dot{\mathbf{g}}_{qf} \quad (6)$$

where

$$\dot{\mathbf{g}}_{qf} \approx -\frac{\Omega}{q_0} \quad (7)$$

where q_0 is the cone angle; the non-Newtonian viscosity is given by

$$\mathbf{h} = \frac{3q_0T}{2pR^3\Omega} \quad (8)$$

The torque (T) is measured and the rotational velocity (Ω) is controlled [1].

Determining rheological properties does not require any assumption about flow kinematics, nor does it require the rheological models. Very small sample volumes are needed. The system allows for very good heat transfer and temperature control. End effects are negligible, at least for low rotational speeds when using the appropriate quantity of fluid in the gap.

While this geometry appears to be ideal for rheological studies, it does have some disadvantages. The system is limited to low shear rates, especially for highly elastic systems which would not stay in the gap at a high rotational speed. It is difficult to eliminate evaporation and free-boundary effects for solutions involving volatile solvents. Highly erroneous results are possible for multiphase systems such as suspensions of solids and polymer blends, in which the particles or domain sizes are of the same order of magnitude as the gap size [1].

Parallel-Plate Geometry. Since the cone and plate geometry may not be ideal for the study of multiphase system and polymer blend rheology, the parallel-plate geometry can be used.

This geometry consists of two parallel concentric discs of radius R with a constant separation or gap. One of the plates rotates and the other remains stationary; the torque and normal thrust can be measured at either plate. The edge represents a free boundary on the measured torque and axial forces are usually negligible. This geometry is advantageous for high temperature measurements, particularly when multiphase systems are studied. The gap can be varied to accommodate a variety of particle sizes.

For a small gap ($h/R \ll 1$), or for low rotational speed, the velocity profile for steady-state conditions is given by

$$V_q = \Omega r \left(1 - \frac{z}{h} \right) \quad (9)$$

and the shear rate ($\dot{\mathbf{g}}_{zq}$) is given by

$$\dot{\mathbf{g}}_{zq} = \Omega \frac{r}{h} \quad (10)$$

Carreau et. al [2], state that for non-Newtonian fluids, the viscosity is no longer proportional to the torque because the shear rate varies with the radial position. The viscosity for non-Newtonian fluids can be expressed by the following equation:

$$h(\dot{\mathbf{g}}_R) = \frac{T}{2pR^3 \dot{\mathbf{g}}_R} \left[3 + \frac{d \ln \left(\frac{T}{2pR^3} \right)}{d \ln \dot{\mathbf{g}}_R} \right] \quad (11)$$

Models for Materials That Exhibit a Yield Stress

Bingham Model. The Bingham model is the simplest one to use because it is a straightforward extension of Newton's law of viscosity:

$$\left\{ \begin{array}{ll} \mathbf{s}_{yx} = -h_0 \dot{\mathbf{g}}_{yx} \pm \mathbf{s}_0 & \text{if } |\mathbf{s}_{yx}| > |\mathbf{s}_0| \\ \dot{\mathbf{g}}_{yx} = 0 & \text{if } |\mathbf{s}_{yx}| \leq |\mathbf{s}_0| \end{array} \right\} \quad (12)$$

The parameters are \mathbf{s}_0 and \mathbf{h}_0 . The model indicates that the sample behaves like a Newtonian material when the shear stress exceeds the yield stress \mathbf{s}_0 , and it doesn't flow when the shear stress is less than the yield stress [1].

Casson Model. The Casson model is given by

$$\sqrt{|\mathbf{s}_{yx}|} = \sqrt{\mathbf{s}_0} + \sqrt{\mathbf{h}_0 |\dot{\mathbf{g}}_{yx}|} \quad (13)$$

A plot of $\sqrt{|\mathbf{s}_{yx}|}$ versus $\sqrt{|\dot{\mathbf{g}}_{yx}|}$ will produce $\sqrt{\mathbf{s}_0}$ as intercept.

Both models introduce a yield stress value; however, the assumption is that the sample behaves as a Newtonian fluid at low shear rates.

Direct Yield Stress Measuring Devices

Vane Technique

One of the direct yield stress measuring devices involves a vane, which generally consists of a small number (2-8) of blades arranged at equal angles around a small cylindrical shaft. In addition to the elimination of wall slip, this geometry can keep any disturbance caused by the introduction of the vane into the sample to a minimum.

A vane test is done by gently introducing the vane spindle into a sample of the suspension held in a container until the vane is fully immersed. The vane is then rotated very slowly at a constant rotational speed, and the torque required to maintain the vane's constant motion is measured as a function of time [14]. From the resulting torque-time curve, the maximum torque that corresponds to the point at which the sample begins to flow can be determined; i.e. the yield stress point. The following correlation between torque and yield stress was derived by Nguyen and Boger [14]:

$$T_m = \frac{\rho D_v^2}{2} \left(\frac{H}{D_v} + \frac{1}{3} \right) \mathbf{s}_0 \quad (14)$$

where T_m is the torque, \mathbf{s}_0 is the yield stress, D_v and H are the dimensions of the vane.

It is assumed that the \mathbf{s}_e (shear stress at the end surface) is uniformly distributed over both end surfaces of the vane and that \mathbf{s}_e is equal to the shear stress $\{\mathbf{s}_w (= \mathbf{s}_{r\theta} |_{r=R_v})\}$. Also, at the maximum torque (T_m), it is assumed that the material yields instantaneously along the virtual cylindrical surface described by the vane rotation, and that the shear stress \mathbf{s}_w is equal to the material yield stress \mathbf{s}_0 .

Slotted plate technique

Setup. A direct yield stress measuring device was constructed by Zhu and De Kee [6]. This instrument, shown in figure 4, employs a slotted plate, which unites the advantages of both vane and solid plate direct yield stress measurements. It is not restricted by the assumptions of the vane method and eliminates the wall effect present with the solid plate method.

The slotted-plate technique consists of a linear motion platform (Applied Motion Products) driven by a step motor (Si3540 programmable step motor driver), a balance (Ohaus, AP250D, capacity

52/210g, resolution 0.01/0.1 mg), and a controlling computer. This computer controls the speed of the platform. A second computer is connected to the balance via a serial connection through the COM1 port for data analysis. A piece of thread hangs from the balance, and a thin stainless steel wire (0.127 mm in diameter) is connected to the thread. This eliminates the torque exerted on the plate, which is connected to the wire, from influencing the balance reading.



Figure 4
Slotted plate set up

Procedure. The samples were stirred by a mixer prior to measurement in order to achieve a similar initial structural state. After the mixing, the asphalt emulsion was loaded into a plastic beaker, placed on the platform, and allowed to rest for two minutes. The slotted plate was suspended from the balance and vertically inserted into the sample at point A in figure 5. A 15-minute rest period at this point allowed the system to equilibrate. A 10- μ l drop of water-soluble surfactant (Tween 85) was placed on the sample surface (point B in figure 5). Once the force versus time curve plateaued (point C in figure 5), the platform was lowered at a controlled and constant rate. As the platform was lowered, the sample in the beaker exerted a force on the plate. This continuously changing force was recorded by the balance and plotted in Excel as a force versus time curve. Once the acting force exceeded the sample yield stress (change in slope), flow began in

the vicinity of the plate, where the stress had the largest magnitude (point D in figure 5). Point C refers to the “initial force” (F_i), and point D is the force (F) at time t_r .

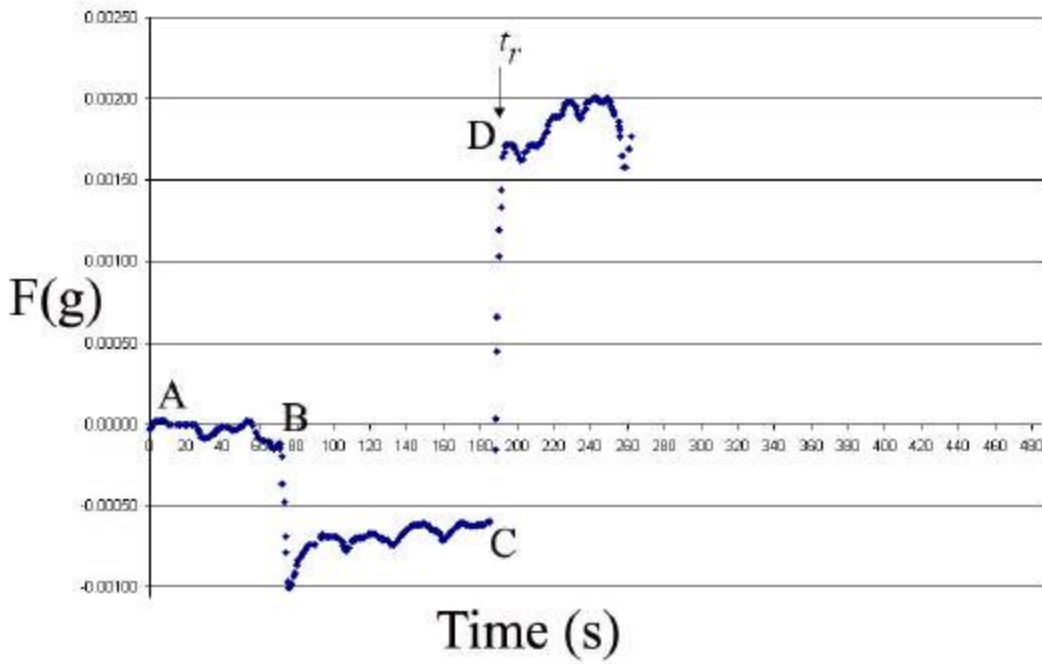


Figure 5
Force - time curve

This point is characterized by a change in slope at $t = t_r$. The yield stress is given by:

$$s_0 = \frac{F_r}{S} = \frac{F - F_i}{S} \quad (15)$$

where S is the total surface area of the plate, F is the total force obtained by the balance at time t_r , and F_i is the measured initial force.

RESULTS AND DISCUSSION

Yield Stress Testing Using a New Slotted Plate Apparatus

Procedure

The sample was first rotated on the CEL-GRO Rotator for at least 24 hours at 7 rpm to ensure the consistency of the sample. The samples used for these tests were stored for an extended period of time and needed to be homogenized before the testing was performed. In a field situation, this step can be neglected because the samples would be homogenized while in transport.

After rotating for 24 hours or more, a sample was poured into a 100 ml beaker and mixed by hand to remove any air bubbles that formed on the surface. The sample was allowed to rest for two minutes before inserting the plate. After the plate was vertically inserted in the sample, the system was allowed to equilibrate. Allowing the sample to rest for 2 and 15 minutes before starting the motor determined the time needed for the emulsion to achieve equilibrium. After inserting the plate, the data collecting software (Winwedge), together with an Excel file, recorded the data from the balance. After the curve plateaued, 10 μ L of surfactant (Tween 85) was added to the sample's surface. The need for surfactant arises when the yield stress of the material is of the same or lower magnitude than the surface tension force at the stainless steel wire – surface interface. The surfactant is a surface acting agent and will stay on the surface of the emulsion if the surfactant concentration is small. We added 10 μ L of surfactant, which is small enough for us to be confident that the surfactant will not interact with the emulsion. After the curve plateaued again, the motor was started (rate of lowering is 0.025 mm/s) and the data was recorded. The results indicated that the surfactant was not necessary. (Note: all tests were performed at 25°C.)

Sample SS-1

The average yield stress was determined to be 0.011 Pa. A 2^n factorial design testing procedure was followed, where $n = 3$ with the mixing time (min.), mixing speed (rpm), and the rest time after mixing (min.) as variables. This factorial design procedure was chosen to determine the effect of the aforementioned variables on the yield stress of the asphalt emulsions. We used an industrial mixer (Silverson L4RT) with variable speed control to mix the sample before the plate was inserted. The yield stress results are given in table 1.

Table 1
Sample SS-1 results

Mixing Time (min.)	Mixing Speed (rpm)	Rest Time after Mixing (min.)	Average Yield Stress (Pa)
2	100	2	0.012
2	100	15	0.011
2	1000	2	0.010
2	1000	15	0.011
15	100	2	0.011
15	100	15	0.010
15	1000	2	0.011
15	1000	15	0.011
Average			0.011

The results show that the mixer had no significant effect on the yield stress of the emulsions. Thus, the rest of the samples were not mixed with the mixer but were mixed by the CEL-GRO Rotator for 24 hours and by hand for two minutes. Again, this mixing procedure will be modified for field testing.

Sample CRS-2

The average yield stress was 0.035 Pa. A 2² factorial design testing procedure was followed, since mixing speed was determined to be of little significance. The variables were rest time after mixing (min.) and rest time (min.) after plate insertion. The yield stress results for sample CRS-2 are given in table 2.

Table 2
Sample CRS-2 results

Rest Time After mixing (min.)	Rest Time After plate insertion (min.)	Yield Stress (Pa)
2	2	0.033
2	15	0.034
15	2	0.035
15	15	0.035
Average		0.035

Sample AES-300

The average yield stress was 0.204Pa. Again, a 2² factorial design testing procedure was followed, since mixing speed was determined to be of little significance. The variables were rest time after mixing (min.) and rest time (min.) after plate insertion. The yield stress results for sample AES-300 are given in table 3.

Table 3
Sample AES-300 Results

Rest Time After Mixing (min)	Rest Time After Plate Insertion (min)	Yield Stress (Pa)
2	2	0.197
2	15	0.204
15	2	0.201
15	15	0.209
Average		0.203

Sample CSS-1

The average yield stress was 0.052 Pa. The procedure outlined for sample CRS-2 was used to determine the yield stress. The yield stress results for sample CSS-1 are given in table 4.

Table 4
Sample CSS-1 results

Rest Time After Mixing (min)	Rest Time After Plate Insertion (min)	Yield Stress (Pa)
2	2	0.050
2	15	0.053
15	2	N/A ¹
15	15	0.054
Average		0.052

¹ The data is unavailable for this test due to the shortage of materials

Sample CRS-2P

The average yield stress was 0.033 Pa. The procedure outlined for sample CRS-2 was used to determine the yield stress. The yield stress results for sample CRS-2P are given in table 5.

Table 5
Sample CRS-2P results

Rest Time After Mixing (min)	Rest Time After Plate Insertion (min)	Yield Stress (Pa)
2	2	0.031
2	15	0.029
15	2	0.033
15	15	0.037
Average		0.033

Sample AE-P

The average yield stress was 0.0016 Pa. The procedure outlined for sample CRS-2 was used to determine the yield stress. The yield stress results for sample AE-P are given in table 6.

Table 6
Sample AE-P results

Rest Time After Mixing (min)	Rest Time After Plate Insertion (min)	Yield Stress (Pa)
2	2	0.0011
2	15	0.0017
15	2	0.0016
15	15	0.0015
Average		0.0015

Analysis and Discussion of Slotted Plate Technique Results

The two-minute rest time after insertion was insufficient for samples CRS-2, CRS-2P, and CSS-1 to achieve a steady state, thus rendering the yield stress determinations inaccurate. Those samples need at least 13 minutes to come to equilibrium. A 15-minute rest period after plate insertion in the sample is sufficient to determine the yield stress accurately.

Table 7
Yield Stress Values for All Samples

	SS-1	CRS-2	AES-300	CSS-1	CRS-2P	AE-P
Yield stress (Pa)	0.011	0.035	0.203	0.052	0.033	0.0016
Average % Error (%)	2.51	1.9	0.87	1.38	5.60	5.83
Standard Deviation	0.0008	0.0011	0.0049	0.0019	0.0052	0.0002

The average yield stress values and percent error for the samples are given in the table 7. The factorial experimental design procedure showed that the mixer speed and time of mixing had no significant effect on the yield stress of sample SS-1. A rest time of two minutes was observed before the insertion of the plate to allow the sample to come to equilibrium. Different rest times after plate insertion did not have a substantial effect on the yield stress for this sample. From the data it is clear that the test can be performed within two minutes after inserting the plate in the sample SS-1.

For sample CRS-2 the variables were the rest time after mixing and rest time after plate insertion. It was assumed that neither the mixing time nor the rate of mixing had a significant effect on the yield stress of the sample. The average percent error for this set of data is 1.9 percent, which is well within an acceptable error range. The rest times after mixing and after plate insertion did not have a

significant effect on the yield stress results. The yield stress results varied less in the longer rest times after plate insertion than in the shorter rest times. This observation suggests that the sample requires more than two minutes to achieve equilibrium. Thus the suggested rest time is at least five minutes for sample CRS-2.

For the rest of the samples, the variables remained the same: the rest time after mixing, and the rest time after plate insertion into the sample. Both variables were tested for two and fifteen minutes following the 2^2 factorial test design. It was found that the two-minute rest time after insertion of the plate was not sufficient for most samples to come to equilibrium, and the rest time before the insertion of the plate into the sample (the time after mixing) had no significant effect on the yield stress determinations of the sample. Different charges on particles in samples CSS-1 and SS-1 would create different structures, leading to different yield stress values. We have noted that CRS-2P is settling faster than AE-P, likely contributing to the larger percent error.

Yield Stress Results Using Rotational Rheometers

Procedure

The sample was prepared as described earlier. The sample was loaded into the TA AR2000 advanced rheometer using a parallel plate or cone and plate geometry, depending on the sample. The CRS-2 samples were tested with parallel plate geometry since the particle size was larger than the minimum gap associated with the cone and plate geometry. The sample was allowed to rest for five minutes before testing. The TA AR2000 software computed the data. Testing via concentric cylinder geometry was performed with a Bohlin 88 viscometer. The sample was loaded into the cap and the rotational cylinder was immersed in the sample. Again, the sample was allowed to rest for five minutes prior to the start of the experiment. All tests were performed at 25° C.

Results Obtained with TA AR-2000 Rheometer

Sample SS-1. The data obtained for the sample SS-1 via the rotational measurements are shown in figure 6. The computed Casson and Bingham yield stress values are shown in table 8, along with the slotted plate results. The extrapolations used the data at the lower values of shear rate. Clearly, using all of the viscometric data for the extrapolation process would result in even larger errors.

Table 8
Sample SS-1 results

	Bingham Yield Stress (Pa)	Casson Yield Stress (Pa)	Slotted Plate Yield Stress (Pa)
Trial 1	0.100	0.012	0.012
Trial 2	0.200	0.063	0.010
Trial 3	0.050	0.012	0.011
Average	0.117	0.029	0.011
Percent Error (%)	24.67	39.79	2.51

The three tests produced three different curves at the low shear rate values; values at low shear rate are required in order to extrapolate to zero shear rate. At higher shear rate values, the three curves converged. The Bingham model assumes Newtonian behavior of the sample, once the sample starts flowing. Note that the SS-1 samples were non-Newtonian fluids, further adding to the difficulties encountered by determining the material yield stress via an extrapolation technique.

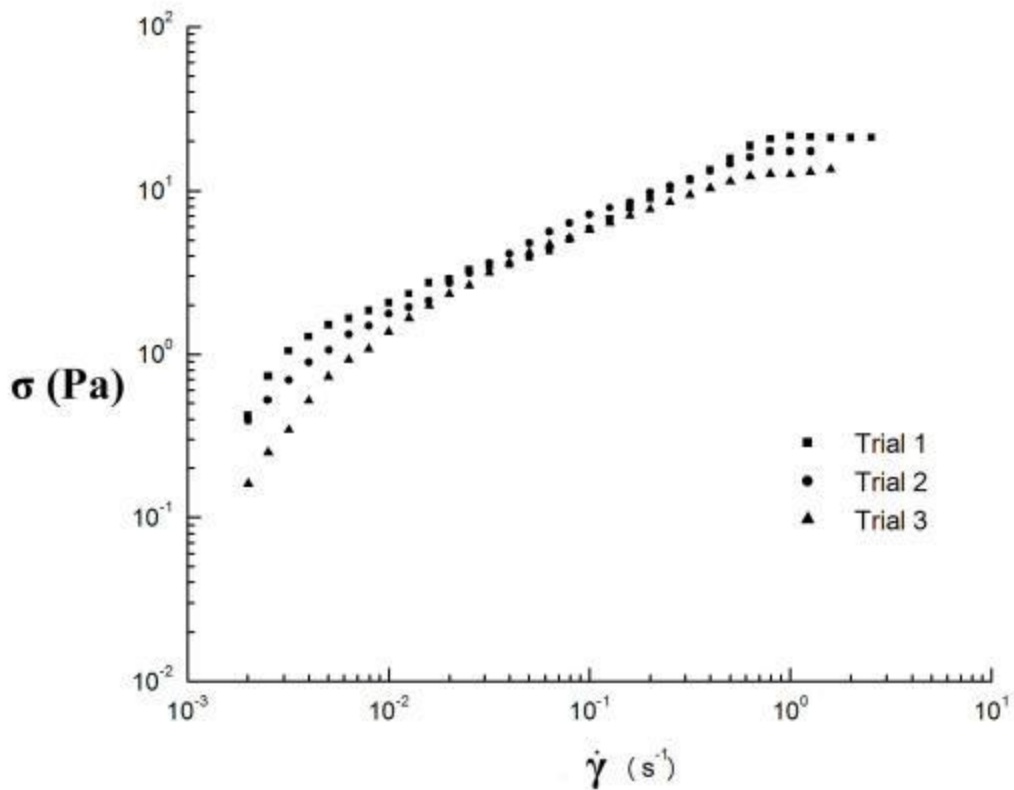


Figure 6
Sample SS-1 results

Sample CRS-2. The data obtained for the sample CRS-2 via the rotational measurements are shown in figure 7. The computed Casson and Bingham yield stress values are shown in table 9, along with the slotted plate results.

Table 9
Sample CRS-2 results

	Bingham Yield Stress (Pa)	Casson Yield Stress (Pa)	Slotted Plate Yield Stress (Pa)
Trial 1	0.130	0.036	0.035
Trial 2	0.150	0.078	0.034
Trial 3	0.450	0.303	0.035
Average	0.243	0.139	0.035
Average Percent Error (%)	27.96	41.23	1.95

The extrapolations used the data at the lower values of shear rate. Clearly, using all of the viscometric data for the extrapolation process would result in even larger errors. Here again, the shear stress response varied greatly from trial to trial in the low shear rate region, which is the region of interest. At higher shear rate values, the curves converged. Clearly, the data from the extremely low shear rate region are not reliable.

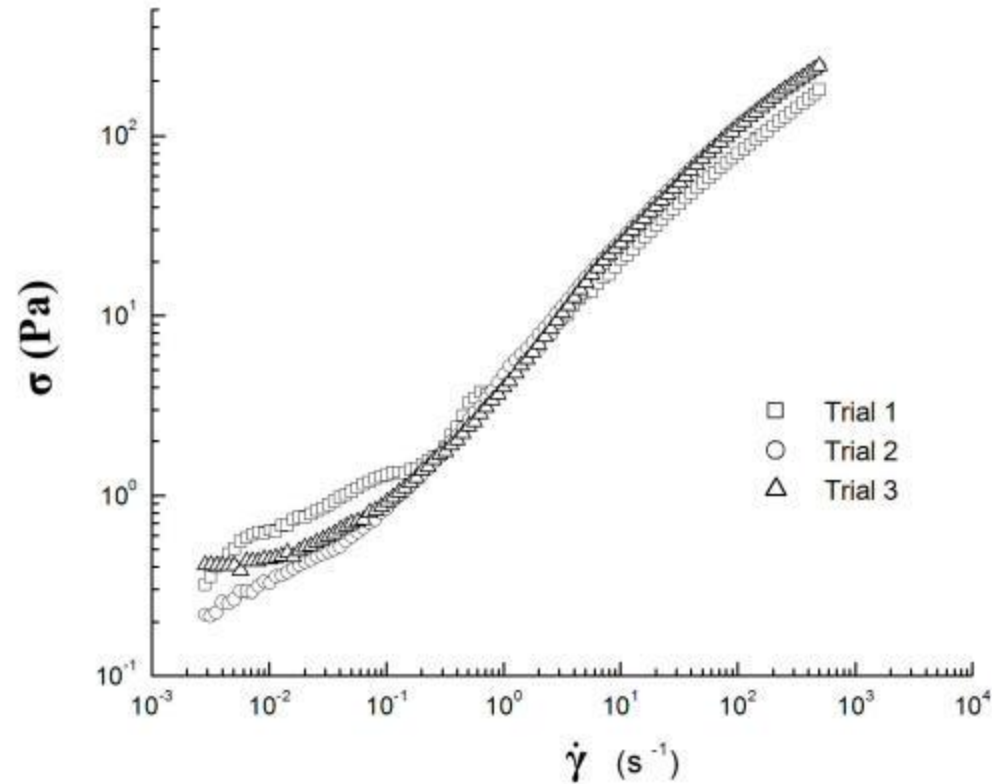


Figure 7
Sample CRS-2 results

Sample AES – 300. The data obtained for the sample AES-300 via the rotational measurements are shown in figure 8. The computed Casson and Bingham yield stress values are shown in table 10, along with the slotted plate results.

Table 10
Sample AES-300 results

	Bingham Yield Stress (Pa)	Casson Yield Stress (Pa)	Slotted Plate (Pa)
Trial 1	0.051	0.040	0.204
Trial 2	1.200	0.160	0.201
Trial 3	0.048	0.036	0.209
Average	0.433	0.079	0.205
Average Percent Error (%)	68.65	34.47	0.705

Again, the extrapolations used the data at the lower values of shear rate. Not surprisingly, the data in the ($<10^{-2} \text{ s}^{-1}$) shear rate region varied greatly from trial to trial; this was no longer true of the higher shear rate values.

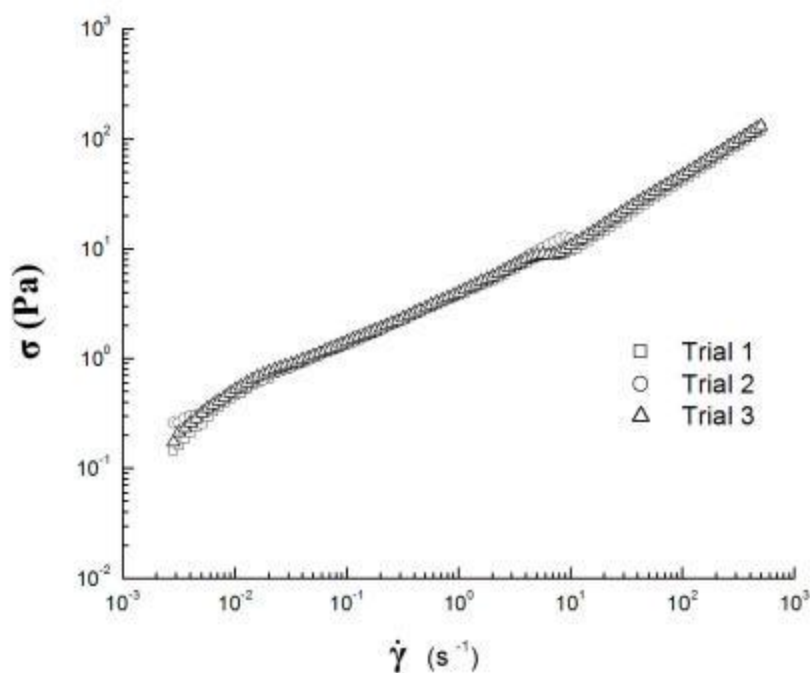


Figure 8
Sample AES-300 results

Sample CSS – 1. The data obtained for the sample CSS-1 via the rotational measurements are shown in figure 9. The computed Casson and Bingham yield stress values are shown in table 11, along with the slotted plate results. Again, the extrapolations used the data at the lower values of shear rate.

Table 11
Sample CSS-1 results

	Bingham Yield Stress (Pa)	Casson Yield Stress (Pa)	Slotted Plate Yield Stress (Pa)
Trial 1	0.007	0.123	0.050
Trial 2	0.020	0.203	0.053
Trial 3	0.014	0.084	N/A
Trial 4	0.006	0.017	0.054
Average	0.012	0.107	0.052
Average Percent Error (%)	17.11	12.72	2.970

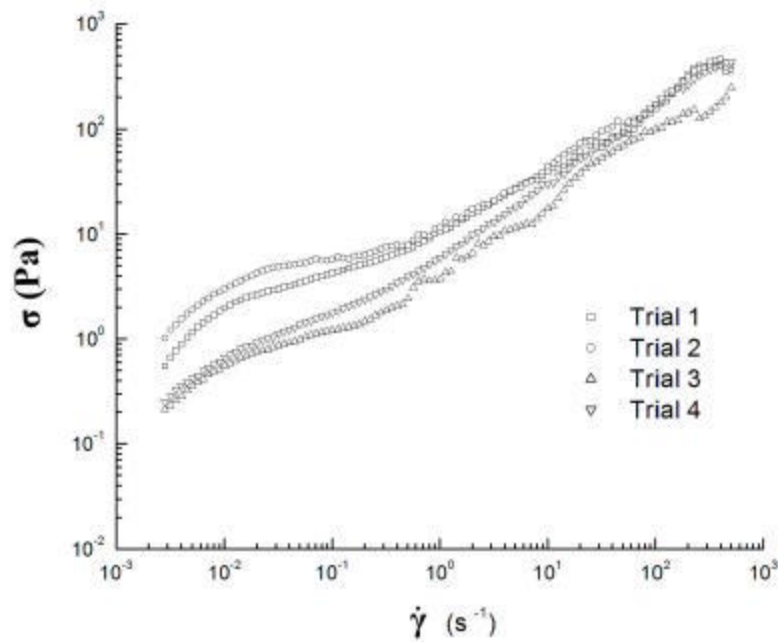


Figure 9
Sample CSS-1 results

Sample CRS – 2P. The data obtained for the sample CRS-2P via the rotational measurements are shown in figure 10. The computed Casson and Bingham yield stress values are shown in table 12, along with the slotted plate results. Again, the extrapolations used the data at the lower values of shear rate, resulting in major differences from the slotted plate experimental results.

Table 12
Sample CRS-2P results

	Bingham Yield Stress (Pa)	Casson Yield Stress (Pa)	Slotted Plate Yield Stress (Pa)
Trial 1	$4.0 \cdot 10^{-5}$	$1.76 \cdot 10^{-07}$	0.031
Trial 2	$3.0 \cdot 10^{-7}$	$1.00 \cdot 10^{-08}$	0.033
Trial 3	$3.0 \cdot 10^{-8}$	$4.00 \cdot 10^{-12}$	0.037
Average	$1.34 \cdot 10^{-5}$	$6.21 \cdot 10^{-08}$	0.034
Average Percent Error (%)	81.63	73.39	3.28

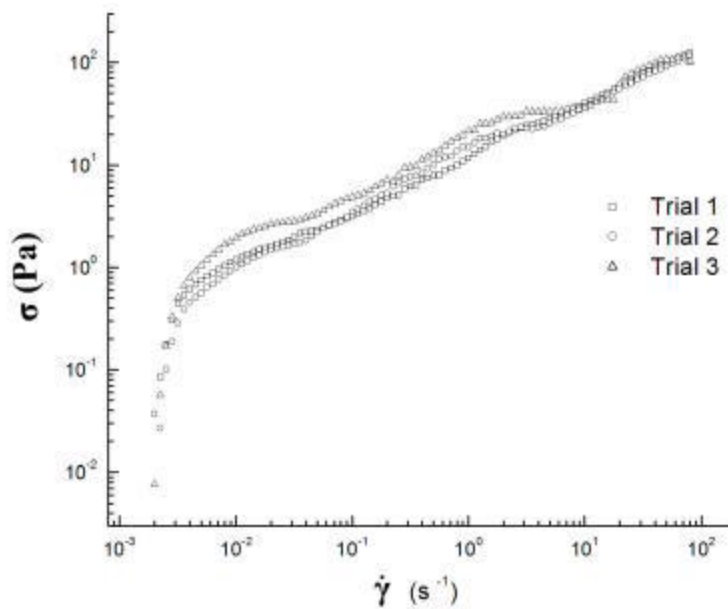


Figure 10
Sample CRS-2P results

Sample AE-P. The data obtained for the sample AE-P via the rotational measurements are shown in figure 11. The computed Casson and Bingham yield stress values are shown in table 13, along with the slotted plate results. Again, the extrapolations used the data at the lower values of shear rate.

Table 13
Sample AE-P results

	Bingham Yield Stress (Pa)	Casson Yield Stress (Pa)	Slotted Plate Yield Stress (Pa)
Trial 1	$6.00 \cdot 10^{-07}$	$1.3 \cdot 10^{-3}$	0.0015
Trial 2	$1.00 \cdot 10^{-08}$	$3.4 \cdot 10^{-4}$	0.0017
Trial 3	$6.00 \cdot 10^{-03}$	$7.5 \cdot 10^{-2}$	0.0016
Average	$2.00 \cdot 10^{-03}$	$2.5 \cdot 10^{-2}$	0.0016
Average Percent Error (%)	83.31	83.27	2.09

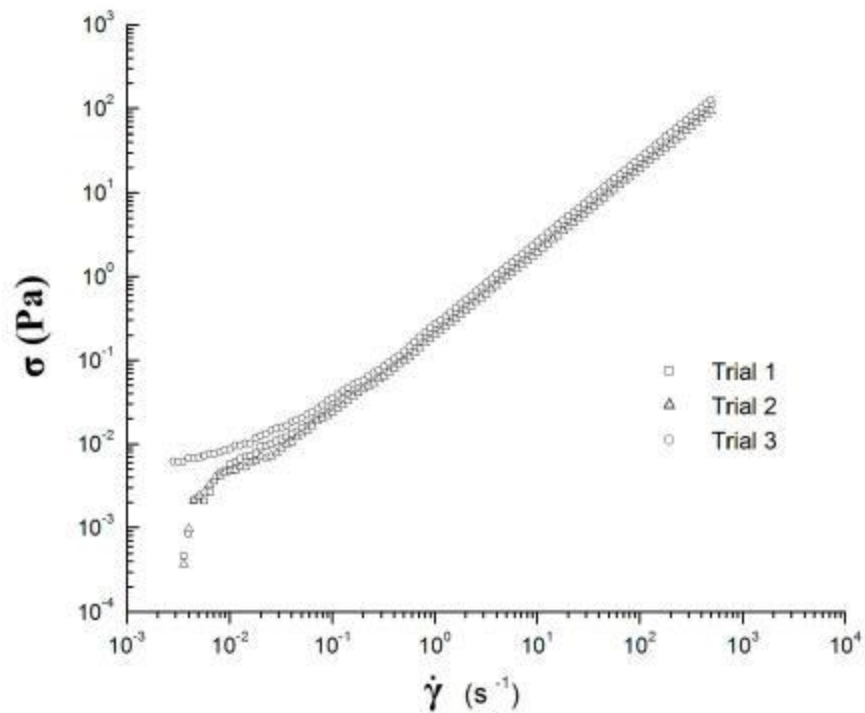


Figure 11
Sample AE-P results

Table 14
Bohlin Visco 88 viscometer results

Trial	SS-1		CRS-2		Slotted Plate (Pa)	
	Bingham (Pa)	Casson (Pa)	Bingham (Pa)	Casson (Pa)	SS-1	CRS-2
1	0.64	0.049	0.029	0.002	0.012	0.035
2	0.58	0.047	0.47	0.009	0.010	0.034
3	0.59	0.052	0.77	0.03	0.011	0.035
Average	0.60	0.049	0.42	0.014	0.011	0.035
Average Percent Error (%)	2.95	0.34	87.2	74.5	2.51	1.95

Trial	AES-300		CSS-1		Slotted Plate (Pa)	
	Bingham (Pa)	Casson (Pa)	Bingham (Pa)	Casson (Pa)	AES-300	CSS-1
1	3.577	1.283	0.0255	0.0005	0.204	0.050
2	4.127	1.239	0.112	0.00125	0.201	0.053
3	3.494	1.239	0.0501	2.5*10 ⁻⁶	0.209	0.054
Average	3.733	1.254	0.0625	0.006	0.205	0.052
Average Percent Error (%)	3.48	0.78	27.15	47.74	0.705	2.970

Trial	CRS-2P		AE-P		Slotted Plate (Pa)	
	Bingham (Pa)	Casson (Pa)	Bingham (Pa)	Casson (Pa)	CRS-2P	AE-P
1	0.268	0.0395	0.2874	0.0095	0.031	0.0015
2	0.131	0.0016	0.2697	0.00897	0.033	0.0017
3	0.922	0.057	N/A	N/A	0.037	0.0016
Average	0.440	0.0327	0.279	0.009	0.034	0.0016
Average Percent Error (%)	37.99	42.39	1.59	1.44	3.28	2.09

Yield Stress Results Obtained with Bohlin 88 Viscometer

The data in table 14 show the yield stress results for all 6 samples obtained with a concentric cylinder geometry used with the Bohlin 88 instrument. This instrument generated data equivalent to data obtained with a Brookfield viscometer.

The Bingham yield stress result was obtained via extrapolation of the $t - \dot{\gamma}$ data (see figure 12) to zero shear rate. Similarly, the Casson yield stress result was obtained via extrapolation of the data as shown in figure 13.

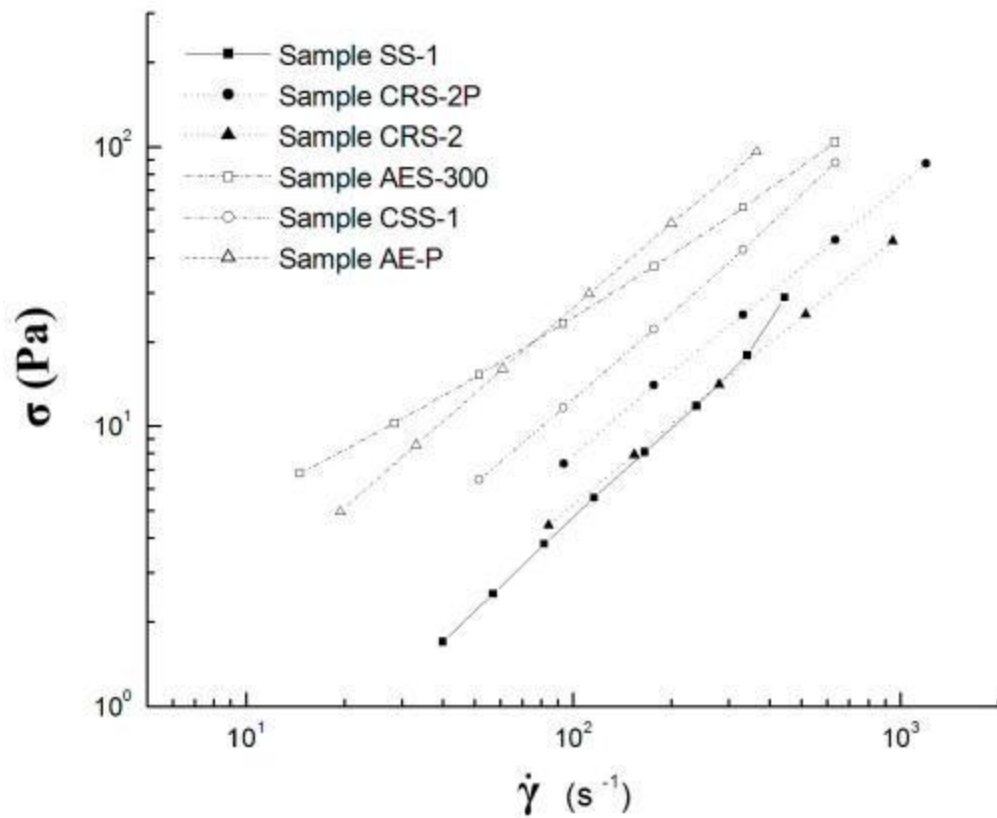


Figure 12
Bingham model curve fit

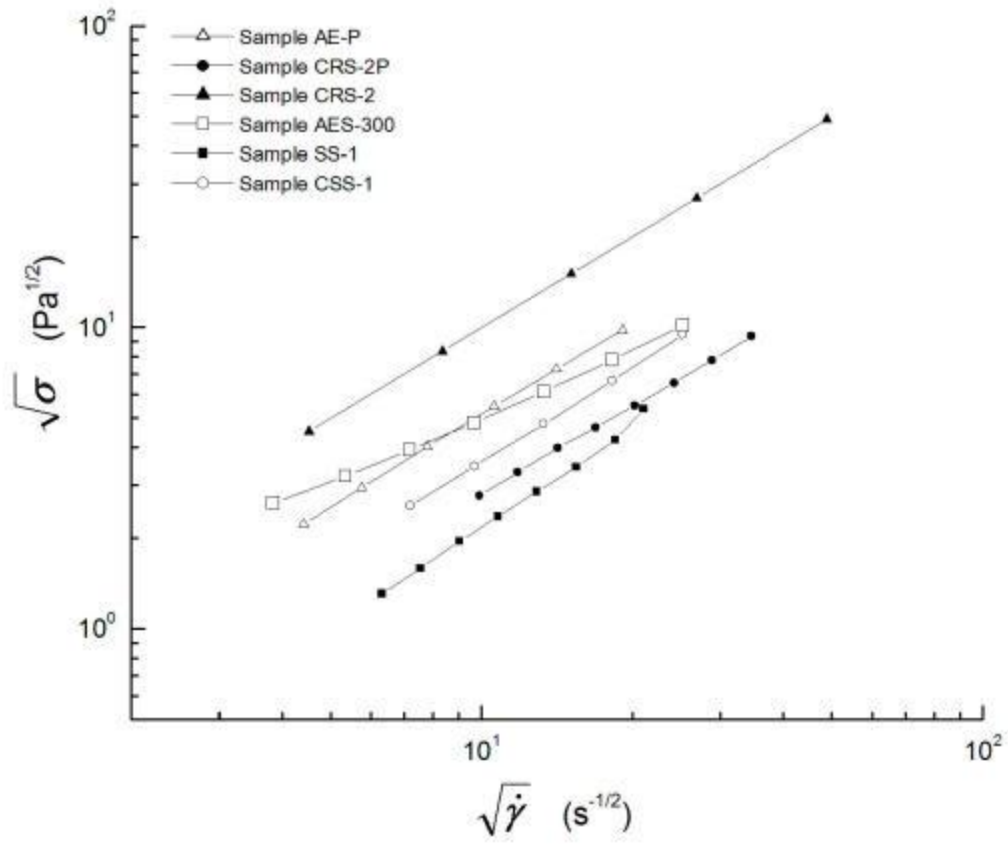


Figure 13
Casson model curve fit

Discussion of Data Obtained via Rotational Rheometers.

The yield stress of asphalt emulsions is difficult to measure with any degree of certainty using the cone and plate or parallel plate geometries. Although the TA AR-2000 rheometer is a top-of-the line research instrument, it is not sensitive enough at the very low shear rate region to produce reproducible data for the shear stress–shear rate relationships, from which the yield stress is obtained via extrapolation. The underlying assumption of the Bingham model is Newtonian behavior of the sample in the flow region. The data prove that the asphalt emulsions do not behave as Newtonian fluids in the low shear rate region. The extrapolation to zero shear rate thus gives inaccurate results.

Table 15
Summary of the results for rotational rheometers and comparison with the slotted plate results

	SS-1	CRS-2	CRS-2P	AES-300	AE-P	CSS-1
TA AR-2000 Results						
Bingham Yield Stress (Pa)	0.117	0.243	$1.34 \cdot 10^{-05}$	0.433	$2.00 \cdot 10^{-03}$	0.012
Casson Yield Stress (Pa)	0.029	0.139	$6.21 \cdot 10^{-08}$	0.079	$2.50 \cdot 10^{-02}$	0.107
Bohlin 88 Results						
Bingham Yield Stress (Pa)	0.60	0.42	0.440	3.733	0.279	0.0625
Casson Yield Stress (Pa)	0.049	0.014	0.0327	1.254	0.009	0.006
Slotted Plate Yield Stress (Pa)	0.011	0.035	0.034	0.205	0.0016	0.0525

The TA AR-2000 advanced rheometer achieved shear rate values as low as 10^{-3} s^{-1} , which provided more confidence in the results obtained via extrapolation. However, even with data at such low shear rate values, the results were inconsistent for the most part. At first sight, one can conclude that the Casson model is better at predicting the yield stress of the asphalt emulsions. At higher shear rates, all of the samples exhibited power law behavior, and at very high shear rates, they exhibited Newtonian behavior, as expected. The curves converged for the shear rate values greater than 10 s^{-1} . The Casson and Bingham models overestimated the true yield stress of the material.

Because the Bohlin Visco 88 viscometer is incapable of attaining low shear rates values

(< 10^0 s^{-1}), it compounds the errors resulting from the extrapolation of the data to the lower shear rate regions. The results of the Bohlin 88 tests are given in table 15. These results indicate that using rotational viscometers at higher shear rates generates reproducible results, but the extrapolations to zero shear rate are highly dependent on the model (Bingham, Casson, etc.) used. Yield stress determinations using rotational geometries followed by extrapolation procedures should be avoided.

Saybolt Viscosity Determination of Asphalt Emulsions

Procedure

The sample was prepared according to the AASHTO T72-97 standard procedure. The water bath for the Saybolt apparatus was established at 25°C, and the sample was preheated to 25°C. The sample was hand stirred and then strained, using number 100 wire cloth in the filter funnel, directly into the viscometer until the level was above the overflow rim. The efflux time was measured using a RadioShack Multifunction LCD Stopwatch to the nearest 0.1 s.

Results

Saybolt testing was performed on the four samples following the AASHTO T 72-97 standard at 25°C using water as a bath medium. The shortage of samples prevented more tests at higher temperatures.

Discussion of Saybolt Measurement Results

The Saybolt viscosity, given in units of (s), is not comparable to the proper viscosity that relates shear stress to shear rate and is expressed in $(Pa \cdot s)$. Note that the viscosity of a complex system, such as an asphalt emulsion, is a function of shear rate. Because we are dealing with a non-Newtonian viscosity, using a “one point viscosity value” as a quality control tool cannot be justified.

The idea of using a single value quality control parameter is appealing. The results of this preliminary research program suggest that the sample yield stress is a good candidate for such a one point measure, as it can be determined within an acceptable error margin. In addition, the concept of a yield stress provides a solid physical basis for this choice of quality control.

Table 16
Saybolt results

Sample	Trial	Efflux Time	Correction Factor	"Viscosity"
CSS-1	1	47.84	1.0546	50.45
	2	55.75	1.0572	58.94
	3	59.28	1.0572	93.19
Average				67.53
AES-300	1	96.43	1.0546	101.70
	2	102.91	1.0546	108.53
	3	112.28	1.0572	118.70
	4	101.3	1.0572	107.09
				111.44
SS-1	1	23.22	1.0572	24.55
	2	23.69	1.0572	25.05
	3	20.5	1.0546	21.6193
	4	25.28	1.0546	26.66
				24.44
AE-P	1	88.5	1.0572	93.56
	2	92.35	1.0572	97.63
	3	92.75	1.0546	97.81
	4	99.69	1.0546	105.13
				100.19
CRS-2	1	525.5	1.0572	555.56
	2	530.7	1.0572	561.06
	3	527.6	1.0546	556.41
	4	535.0	1.0546	564.21
				559.31
CRS-2P	1	620.1	1.0572	655.57
	2	618.2	1.0572	653.56
	3	625.9	1.0546	660.07
	4	627.3	1.0546	661.55
				657.69

CONCLUSIONS

To our knowledge, no yield stress measurements have been reported for asphalt emulsions. In fact, little attention has been given to any material with low yield stress values [15]. Measuring such low values of yield stress is difficult using traditional methods. The slotted-plate technique accurately determined the yield stress of these emulsions. Other accepted standard tests were performed for comparison. Yield stress measurements obtained via extrapolation of shear stress-shear rate data are definitely not reliable. Another disadvantage of the standard (extrapolation) testing methods is the fact that the yield stress determinations also rely on the choice of a rheological model.

The Saybolt test provides a single viscosity value for a given temperature; however, the emulsions are not Newtonian fluids at lower temperatures. In addition the Saybolt viscosity does not have the units of viscosity, so a viscosity function (curve) is required to express the sample viscosity. Determining a single viscosity point for a non-Newtonian material does not characterize the material. On the other hand, the static yield stress for a particular material is a constant. Thus, this static yield stress determination is preferable as a quality control parameter for asphalt emulsions, provided its value can be obtained within an acceptable magnitude of error.

The purpose of this project was to begin comparing several techniques for determining the yield stress of asphalt emulsions. The project also tested the ability of the slotted plate technique to determine of the yield stress values of asphalt emulsions. Six samples of asphalt emulsions were characterized using concentric cylinders, parallel plate and cone and plate geometries (i.e. rotational rheometers), a slotted plate technique, and a Saybolt viscometer. Results show that the slotted plate technique is superior (i.e. no extrapolation is involved) to the rotational rheometers because it is a direct measurement technique that measures the yield stress in undisturbed samples by carefully inserting the plate in the sample and allowing the sample to come to equilibrium. The slotted plate yield stress results were consistent.

The rotational rheometers did not allow for a direct measurement of the yield stress, as extrapolation of rheometric data was required. The yield stress values obtained via the Casson model were comparable to the slotted plate technique results. The Bingham model did not always predict the yield stress accurately.

The Bingham and Casson yield stresses were determined using a select range of shear rates (lowest possible) from the data obtained with the TA-AR 2000 rheometer. As mentioned earlier, the data were inconsistent at shear rates below 1 s^{-1} .

The Saybolt testing was performed following the AASHTO T 72-97 standard at 25°C. The results from Saybolt testing are not directly comparable to the yield stress results because the Saybolt viscosity is a measure of the time required for 60 ml of emulsion to flow through a capillary, whereas the yield stress is a measure of the stress necessary to induce the flow in the material. However, both of those values are appealing since they are single point characterization parameters. While a single point characterization is practical, such a characterization must be based on solid scientific principles. This is not the case for the Saybolt measurement since the $h - \dot{g}$ relationship is not considered.

The static yield stress determined via the slotted plate technique was a constant. Consistent results within 6 percent error were obtained. The slotted plate technique deserves further investigation involving an expanded array of industrially important emulsions to determine the effects of asphaltene interactions and emulsifying agents on the yield stress. Other variables of interest include the thermal dependence of the yield stress as well as Oswald ripening effects. The ultimate goal of such research would be to establish a new standard procedure to characterize asphalt emulsions.

From a rheological standpoint, the yield stress grading is preferable to the other techniques described in this report. Until now determining the precise yield stress value of the emulsions of interest was nearly impossible, since the yield stress is of a rather small magnitude. Current results suggest that with the slotted plate technique, the static yield stress of asphalt emulsions can be determined with confidence.

NOTATION

Ca	Capillary Number
D_v	vane diameter (m)
F	orifice calibration constant
F_i	“Initial force” (Pa)
F	force at time t_r (Pa)
h	gap between two plates (m)
H	vane height (m)
M	viscosity ratio of the dispersed to the suspending fluids
r	radial position
R	radius of the cone (m)
R	radius of the vane (m)
t	efflux time (s)
t_r	time at which flow is initiated (s)
T	torque (N·m)
T_m	maximum torque (N·m)
S	plate surface area (m ²)
z	axial position

Greek Letters

f	volume fraction
u	saybolt “viscosity” (SFS)
q_0	cone angle (rad or deg)
$\dot{\underline{\underline{g}}}$	rate of deformation tensor $\{ = \underline{\nabla}v + (\underline{\nabla}v)^+ \}$
$\dot{\underline{\underline{g}}}_{rz}, \dot{\underline{\underline{g}}}_{qf}, \dot{\underline{\underline{g}}}_{yx}$	shear rate (s ⁻¹)
$\dot{\underline{\underline{g}}}_R$	wall-shear rate in Poiseuille flow (s ⁻¹)
$\underline{\underline{s}}_{rq}$	(r -?) component of shear stress tensor $\underline{\underline{s}}$
$\underline{\underline{s}}$	stress tensor
$\underline{\underline{s}}_0$	yield stress (Pa)
$\underline{\underline{s}}_e$	end surface shear stress (Pa)
$\underline{\underline{s}}_w$	wall shear stress $\{ = \underline{\underline{s}}_{rq} _{r=R_v} \}$ (Pa)
$\underline{\underline{s}}_{xy}, \underline{\underline{s}}_{qf}$	shear stress (Pa)
Γ	surface tension of the solvent (N·m ⁻¹)
Ω	angular velocity (rad/s)
η	viscosity of the suspension (Pa·s)
h_0	Newtonian viscosity (constant) (Pa·s)
h_r	relative viscosity (Pa·s)
h_s	viscosity of the solvent (Pa·s)

REFERENCES

1. Carreau, P., De Kee, D. and Chhabra, R., *Rheology of Polymeric Systems*. Hanser, New York, 1997.
2. Larson, R., *The Structure and Rheology of Complex Fluids*. Oxford University Press, New York, 1999.
3. Goto, H. and Kuno, H. "Flow of Suspensions COntaining Particles of Two Different Sizes Through a Capillary Tube." *Journal of Rheology*, Vol. 36, No. 5, 1982, 387-398.
4. Hoffman, R. "Factors Affecting The Viscosity of Unimodal And Multimodal Colloidal Dispersions." *Journal of Rheology*, Vol. 36, No. 5, 1992, 947-964.
5. Van Der Werff, J. C. and De Kruff, C. G. "Hard-Sphere Colloidal Dispersions: The Scaling of Rheological Properties With Particle Size, Volume Fraction, and Shear Rate." *Journal of Rheology*, Vol. 33, No. 3, 1989, 421-454.
6. Zhu, L., "A Slotted Plate Device to Measure Yield Stress," PhD dissertation, Tulane University, New Orleans, 2001.
7. The Surfactants Virtual Library, March 26, 2003, <http://www.surfactants.net/emulsion.htm>.
8. AEMA, Asphalt Emulsion Manufacturers Association. Frequently Asked Questions, N.d., June, 9, 2003, <http://www.aema.org/FAQ.htm>.
9. Kenedy, W. T. and Cominsky, J. R., "Hypothesis and Models Employed in the SHRP Asphalt Research Program." Strategic Highway Research Program, Washington D.C., 1990.
10. Bahia, H. U., Hanson, D. I., Zeng, M., Zhai, H., Khatri, M. A. and Anderson, R. M., "Characterization of Modified Asphalt Binders in Superpave Mix Design," NCHRP Report 459, National Academy Press, Washington, D.C., 2001.
11. Deshpande P, V. S., Shahanawaz A. and M.V. Arum, "Microstructure Related Rheological Behavior of Asphalt,," Indian Institute of Technology, Madras, Chennai, India, 2003.

12. Asphalt Emulsions, Ergon, Inc., June, 9, 2003,
http://www.ergon.com/html/asphalt_emulsions.html.
13. Koch Pavement Solutions, Koch Material Company, June, 9, 2003,
<http://www.kochpavementsolutions.com/Solutions/emulsions.htm>.
14. Nguen, D. Q. and Boger, D. V. "Yield Stress Measurement for Concentrated Suspensions." *Journal of Rheology*, Vol. 27, No. 4, 1983, 321-349.
15. Zhu, L., Sun, N., Papadopoulos, K. and De Kee, D. "A Slotted Plate Device for Measuring Static Yield Stress." *Journal of Rheology*, Vol. 45, No. 5, 2001, 1105-1122.